Assessment of various formulation approaches for the application of beta-lapachone in prostate cancer therapy

Xiao Wu, Athena Kasselouri, Juliette Vergnaud-Gauduchon, Véronique Rosilio

Assessment of various formulation approaches for the application of beta-lapachone in prostate cancer therapy

Xiao Wu[1], Athena Kasselouri[2], Juliette Vergnaud-Gauduchon[1], Véronique Rosilio[1*]

[1] Université Paris-Saclay, CNRS, Institut Galien Paris Saclay, 92296, Châtenay-Malabry, France.

[2] Université Paris-Saclay, Lip(Sys)[2], Chimie Analytique Pharmaceutique, 92296, Châtenay-Malabry, France.

* To who correspondance should be addressed: veronique.rosilio@universite-paris-saclay.fr

Abstract

Beta-lapachone (β-Lap) is an anticancer drug activated by the NAD(P)H quinone acceptor oxidoreductase (quinone) (NQO1), an enzyme over-expressed in a large variety of tumors. B-Lap is poorly soluble in water and in most biocompatible solvents. Micellar systems, liposomes and cyclodextrins (CDs) have been proposed for its solubilization. In this work, we analyzed the properties and *in vitro* efficacy of β-Lap loaded in polymer nanoparticles, liposome bilayers, complexed with sulfobutyl-ether (SBE)- and hydroxy-propyl (HP)-β cyclodextrins, or double loaded in phospholipid vesicles. Nanoparticles led to the lowest drug loading. Encapsulation of [β-Lap:CD] complexes in vesicles made it possible to slightly increase the encapsulation rate of the drug in liposomes, however at the cost of poor encapsulation efficiency. Cytotoxicity tests generally showed a higher sensitivity of NIH 3T3 and PNT2 cells to the treatment compared to PC-3 cells, but also a slight resistance at high β-Lap concentrations. None of the studied β-Lap delivery systems showed significant enhanced cytotoxicity against PC-3 cells compared to the free drug. Cyclodextrins and double loaded vesicles, however, appeared more efficient drug delivery systems than liposomes and nanoparticles, combining both good solubilizing and cytotoxic properties. Ligand-functionalized double loaded liposomes might allow overcoming the lack of selectivity of the drug.

Keywords: beta-lapachone, double loaded liposome, cyclodextrin, poly-lactide, PC-3 cell, NQO1.

1. Introduction

Beta-lapachone (3,4-dihydro-2,2-dimethyl-2H-naphthol-[1,2-b]pyran-5,6-dione, β-Lap) is an *ortho*-naphthoquinone extracted from the bark of *Tabebuia avellanedae*. It has drawn strong interest for its wide variety of potential pharmacological effects including anti-tumor activity (Abreu et al. 2005; Kung et al. 2008; Tseng et al. 2013; Ma et al. 2015; Moreno et al. 2015). It has been suggested that β-Lap enters the cancer cells in its oxidized form and is activated after reduction by the NAD(P)H quinone acceptor oxidoreductase (quinone) (NQO1), a multifunctional antioxydant enzyme predominately located in the cytoplasm. This enzyme is overexpressed in a variety of human cancers. Its activity is considered as a key determinant for β-Lap-mediated apoptosis and cytotoxicity in prostate cancer cells, and its expression can be stimulated by the drug itself (Planchon et al. 2001; Kumi-Diaka 2002; Lee et al. 2005; Blanco et al. 2007). The reduced form of β-Lap is unstable leading to the formation of reactive oxygen species (ROS). ROS attack DNA causing cellular stress capable of activating the p53 protein and the expression of the Bax gene. The Bax protein triggers the release of intracellular calcium from the endoplasmic reticulum by interacting with the cytosolic domains of calcium channels. The release of intracellular calcium is also provoked by the depletion of NADH/NADP and ATP due to the overconsumption of the enzyme NQO1. Intracellular calcium release induces apoptosis *via* permeabilization of mitochondrial membranes and release of cytochrome c. It follows the activation of the calpain and caspase pathways leading to cell death. The oxydative pathway to apoptosis also includes mechanisms leading to cell cycle arrest (Kung et al. 2008). Despite its long known therapeutic potential, β-Lap has still no clinical application today. This is mainly due to its low bioavailability, photodecomposition and rapid metabolism once in the blood. Some clinical studies also revealed a certain toxicity. B-lap is poorly soluble in water (0.16 mM or 0.038 mg/mL) (Nasongkla et al. 2003) and in most biocompatible solvents. Approaches that could improve

its solubility and stability include the use of micellar systems and cyclodextrins (CD). Whereas β-Lap solubilization in polymer micelles proved insufficiently effective (Blanco et al. 2007), formation of inclusion complexes with cyclodextrins increased β-Lap stability and bioavailability (Nasongkla et al. 2003; Cunha-Filho et al. 2007; Mangas-Sanjuan et al. 2016; Xavier-Junior et al. 2017). It was shown that the hydrophobic interaction between β-Lap and the apolar cavity of a CD molecule was the main driving force for the formation of inclusion complexes. The complex formed by β-Lap and 2-hydroxypropyl-β-cyclodextrin (HP-β-CD) allowed increasing 413-fold β-Lap water solubility from 0.16 mM to 66.0 mM (Nasongkla et al. 2003), but the most effective candidates for β-Lap solubilization appeared to be the SulfoButyl-Ether (SBE) and Randomly Methylated (RM) β-cyclodextrins (Cunha-Filho et al. 2007; Mangas-Sanjuan et al. 2016; Xavier-Junior et al. 2017). However, inclusion of β-Lap in cyclodextrins does not limit its degradation, although Cunha-Filho et al. (2013) reported the protection of the drug by RM-β-CD against hydrolytic process in darkness. Also, methemoglobinemia and hemolysis were observed with [β-Lap:hydroxypropyl-β-cyclodextrin] complex formulations used in clinical trials (Hartner et al. 2007). Encapsulation of a lipophilic and unstable drug into liposomes is another way to improve its water solubility and limit its degradation. Liposomes can encapsulate hydrophilic drugs in their aqueous core and lipophilic drugs in their phospholipid bilayers. Due to its hydrophobicity, β-Lap intercalates between phospholipid acyl chains in vesicle bilayers (Wu et al. 2019). B-Lap was encapsulated in liposomes made of a mixture of epikuron®200, cholesterol and stearylamine (7:2:1) with 97% encapsulation efficiency (EE) (Cavalcanti et al. 2011). Epikuron®200 mostly consists of 1,2-dilinoleoyl-*sn*-glycero-3-phosphocholine (DLOPC), a poly-unsaturated phospholipid. Stearylamine (SA) is expected to limit vesicles aggregation thanks to its positive charge, destabilize endosomes (Roseanu et al. 2010), produce deformable vesicles and increase drug permeability (Maestrelli et al. 2010). When β-Lap was complexed with HP-

β-CD and encapsulated into the liposomes, the EE was similar as without cyclodextrin (Calvacanti et al. 2011), as if encapsulation efficiencies in the lipid bilayer or the aqueous core of vesicle could be identical. This was intriguing. In this work, we studied the interfacial behavior of β-Lap in mixtures with lipids, its insertion in liposome bilayers and polymer nanoparticles, its complexation with cyclodextrins and the encapsulation of [β-Lap:CD] complexes in lipid vesicles. We analyzed the properties of the various studied systems and their *in vitro* cytotoxicity on prostate epithelial and cancer cells.

2. Materials and methods

2.1. Materials

Beta-lapachone (3,4-dihydro-2,2-dimethyl-2H-naphthol-[1,2-b]pyran-5,6-dione, Mw = 242.27 g/mol) was a gift of Prof. Nereide Santos-Magalhaes (Federal University of Pernambuco, Recife, Brazil) (Figure 1). 1,2-dilinoleoyl-*sn*-glycero-3-phosphocholine PC(18:2/18:2) (DLOPC, M_W = 782.08 g/mol) and 1-palmitoyl-2-oleoyl-sn-glycero-3-phosphocholine (POPC) were purchased from Avanti Polar Lipids, Inc. (Alabaster, AL, USA), and poly (D,L)-lactic acid (PLA) (Resomer R202H®, Mw = 10,000-18,000 g/mol) from Boehringer Ingelheim (Ingelheim am Rhein, Germany). Cholesterol, stearylamine, 4-(2-hydroxyethyl)-1-piperazine-ethanesulfonic acid (HEPES, 99.5% pure), sodium chloride (NaCl, 99% pure), tetrahydrofuran (≥ 99.9% pure), ammonium molybdate (VI) tetrahydrate (81-83% pure), L-ascorbic acid (99% pure), phosphorus standard solution and hydrogen peroxide (30 wt%) were provided by Sigma Aldrich (St. Louis, MI., USA). The reagents for quantification of the enzyme NQO1 in prostate cell lines included: Mini-PROTEAN® TGX™ Gel, 12 well, 20µL, Clarity™ Western ECL Substrate, 2X Laemmli sample buffer and 2-mercaptoethanol (Bio-Rad, USA), RIPA buffer R0278-50mL and protease inhibitor cocktail P8340-1mL (Sigma-

Aldrich), BCA reagent A and B, Anticorps NQO1 (A180): sc-32793(Santa Cruz Animal Health) and Goat anti-mouse IgG human ads-HRP (Southern Biotech, Birmingham, USA), protein ladder plus prestained, Tris glycine SDS buffer solution 10X and Tris glycine buffer solution 10X (Euromedex, Strasbourg), PVDF Transfer membrane (Immobilon®-P, USA) with 0.45µm pore size, Pierce™ BCA protein Assay kit (Thermo scientific, Rockford, USA), and skimmed milk powder (Régilait, France). Sulfobutyl ether-β-cyclodextrin (SBE-β-CD, DS = 6.4) was a gift from Cyclolab (Budapest, Hungary), and 2-hydroxypropyl-β-cyclodextrin (HP-β-CD) was obtained from Sigma-Aldrich. Spectroscopic grade chloroform and methanol (> 99.80% pure) were Carlo Erba reagents. The ultrapure water obtained from the Millipore Milli-Q® Direct 8 water purification System was used for preparing buffer solutions (10 mM HEPES, 150 mM NaCl, pH 7.4).

2.2. Methods

2.2.1. Surface pressure measurements

Surface pressure-surface area (π-A) measurements of lipid monolayers in the absence or presence of the drug were performed using a thermostated Langmuir film trough (775.75 cm^2, Biolin Scientific, Finland) enclosed in a plexiglas box, protected from light. All experiments were performed at 21 ±1°C. Prior to monolayer deposition, the buffer subphase was cleaned by suction. Phospholipids and the drug in a chloroform and methanol (9:1 v/v) mixture were spread at the air/buffer interface, and the system was left for 15 min to allow complete evaporation of the organic solvents. Monolayer compression was then performed at 5 $Å^2.molecule^{-1}.min^{-1}$ speed. Compression cycles included a first compression of monolayers up to 30 mN/m followed by a full expansion and a second complete compression. Results are

mean values of at least 3 measurements. The surface compressional moduli (C_s^{-1}) of monolayers were calculated from the equation (1):

$$C_S^{-1} = -A\frac{d\pi}{dA} \quad (1)$$

where A is the molecular area, and dπ the surface pressure change. Excess free energies of mixing were calculated from equation (2):

$$\Delta G^{exc} = \int_0^{\pi}\left(A_{12}^{exp} - X_1A_1 - X_2A_2\right)d\pi \quad (2)$$

with A_{12}^{exp}-X_1A_1-X_2A_2 the excess molecular area (ΔA^{exc}), A_{12}^{exp} the experimental mean molecular area in the mixed monolayer, A_1 and A_2 the molecular areas of the pure components 1 and 2, and X_1 and X_2 the molar fractions of the two components in the mixed film.

2.2.2. Liposome preparation and characterization

Liposomes were prepared by the thin film hydration method (Bangham 1965). Beta-lapachone (10 mol% of the total mixture amount) and the lipids (pure POPC or POPC-CHOL-SA 7:2:1 molar ratio) were dissolved in a mixture of chloroform and methanol (9:1 v/v). The solvents were evaporated under reduced pressure for 2 h at 45°C yielding a thin lipid-β-Lap film. Then 1 mL buffer, containing or not the cyclodextrins, was added to the thin film to obtain 4 to 10 mM lipid suspension. Vesicles were formed by submitting the lipid-β-Lap suspension to 5 min heating at 45°C, 5 min vortexing, and 5 min sonication at 40°C. Downsizing was performed either by extrusion 21 times through a 200 nm pore-sized polycarbonate membrane by means of a mini-extruder (Avanti Polar Lipids, Inc.) at room temperature, or tip sonication in ice bath using a probe sonicator Vibracell 75041 (750 W, 20

kHz, Bioblock Scientific, Aalst, Belgium) at 20% amplitude. A series of 10 sec-on/5 sec-off cycles were applied for 30 min. All obtained β-Lap-loaded vesicle suspensions were stored at 4°C, in darkness.

The hydrodynamic diameter and zeta potential (ζ) of the obtained vesicles were measured by dynamic light scattering (DLS), and laser doppler electrophoresis, respectively, using a zetasizer Nano ZS90 (Malvern), after dilution of the liposome suspension. Measurements were carried out in triplicate at 21 ±1°C. The morphology of the vesicles was analyzed by cryogenic transmission electron microscopy (cryo-TEM) using a JEOL 2200FS (JEOL USA, Inc., Peabody, MA, U.S.A.) equipped with a Gatan Ultrascan 2K camera (Gatan, Evry, France). Samples were diluted to 1 mg/mL in 1 mM NaCl solution and 5 µL of the suspensions were deposited onto a perforated carbon-coated, copper grid (TedPella, Inc.). After removal of the excess liquid with a filter paper, the grid was quickly frozen in a liquid ethane bath at -180°C and mounted on the cryo holder for microscopic analysis.

2.2.3. Formation of [β-lapachone:cyclodextrin] inclusion complexes and double loaded vesicles

Based on the study by Xavier-Junior et al. (2017), [β-Lap:CD] inclusion complexes were prepared using HP-β-CD and SBE-β-CD in a 1:8 and 1:4 β-lapachone:CD molar ratio, respectively. The β-Lap solution in methanol went through a 30 min nitrogen purging and was freeze-dried to form a thin film. This film was then hydrated with 2.5 mL of aqueous CD solution. The obtained dispersion was sonicated for 30 min, and then submitted to 16 h magnetic stirring at 1.5 *g,* at 25 ± 1°C. The obtained [β-Lap:CD] solution was filtered through a 0.2 µm membrane filter (Millipore) to remove the non-solubilized drug. The samples were freeze-dried prior to β-Lap assay and characterization of the inclusion complexes.

178 Encapsulation of [β-Lap:CD] complexes was performed following two protocols: (i) free CDs
179 were added to a POPC film containing 10 mol% β-Lap; (ii) freeze-dried [β-Lap:CD]
180 complexes were dissolved in buffer and added to a POPC film containing 10 mol% β-Lap.
181 Free β-Lap was removed by ultracentrifugation.

182

183 *2.2.4. Encapsulation of β-Lap in PLA nanoparticles*

184 Poly (D, L)-lactic acid nanoparticles (PLA NPs) were prepared by nanoprecipitation. A
185 solution of PLA and β-Lap in acetone was added dropwise to ultrapure water under moderate
186 magnetic stirring. Acetone was evaporated under reduced pressure. The final suspension was
187 filtered through a 1 µm pore-sized membrane (Glass acrodisc®, Waters) and centrifuged 3
188 times at 3,000 *g* for 15 min at 15 °C to separate free β-Lap. The pellet was suspended in water
189 at the final concentration of 2 mg/mL.

190

191 *2.2.5. B-lapachone and lipid assays*

192 B-lapachone assay was performed at 256 nm by UV-visible spectroscopy using a CARY 300
193 Bio UV-Visible spectrophotometer (Varian, USA). All samples were freeze-dried (for
194 weighing) then dissolved in a mixture of buffer/methanol/THF (0.2:0.8:1). At the studied
195 wavelength, neither the polymer nor the lipids interfered with drug absorbance. Standard
196 calibration curves were obtained with β-Lap concentrations ranging from 5×10^{-6} to 3.5×10^{-5}
197 M in a mixture of methanol and buffer. POPC was quantified using the phosphorus
198 quantitative method described by Chen et al. (1956). All assays were performed in triplicate.

199

200 *2.2.6. Determination of the loading efficiency of liposomes and cyclodextrins*

201 The freeze-dried [β-lap:CD] complexes were accurately weighed and dissolved in methanol
202 before β-Lap assay. The encapsulation rate (ER) and encapsulation efficiency (EE) of β-Lap
203 (Equations 3 and 4) were determined after centrifugation of vesicle or nanoparticle
204 suspensions at 100,000 *g*, at 4°C for 1h to remove the unentrapped drug. The pellet was
205 disrupted by a HEPES buffer/methanol/THF (0.2:0.8:1 v/v/v) solution for nanoparticles and
206 liposomes without CDs, and by HEPES buffer/methanol (1:25 v:v) for liposomes containing
207 CDs, because THF was incompatible with CDs (a white precipitate was formed). The
208 absorbance of the pellet solution and of pure β-Lap diluted in the same solvent mixture was
209 measured at 256 nm. The encapsulation rate (ER) and encapsulation efficiency (EE) were
210 calculated using Equations (3) and (4):

211 $$\mathrm{ER} = \frac{[\beta-Lap]_{pellet}}{[excipient + \beta-Lap]} \times 100 \qquad (3)$$

212 $$\mathrm{EE} = \frac{[\beta-Lap]_{pellet}}{[\beta-Lap]_{initial}} \times 100 \qquad (4)$$

213

214 *2.2.7. Cell culture*

215 Prostate adenocarcinoma cells PC-3 derived from metastatic bone were purchased from
216 ATCC® CRL-1435™, and SV40 immortalized-normal human prostate epithelium cells
217 (PTN2) from Sigma-Aldrich. Fibroblast from mouse embryo (NIH 3T3) were obtained from
218 ATCC® CRL-1658™. PNT2 et PC-3 cells were cultured in RPMI 1640 medium (Roswell
219 Park Memorial Institute medium, Sigma-Aldrich) and NIH 3T3 in DMEM (Dulbecco's
220 Modified Eagle Medium, Sigma-Aldrich), supplemented with 10% fetal bovine serum
221 (Gibco® by Life Technologies™) and 0.5% penicillin-streptomycin (Sigma-Aldrich) in
222 humidified atmosphere containing 5% CO_2 at 37°C.

223

224 *2.2.8. Expression of NQO1 in prostate cells*

225 Western blot analysis of NQO1 expression was performed as described by Lamberti et al.
226 (2013) with some modifications. About 2 million cells par line were treated with 100 µL of a
227 mixture of RIPA buffer and protease inhibitor cocktail (9:1 v/v). After 30 minutes incubation
228 in ice (vortexing every 10 min), non-soluble materials were eliminated by centrifugation
229 (5000 *g*, 5 min). Aliquots of soluble fractions containing 30 µg of total proteins (quantified by
230 bicinchoninic acid assay, Thermo Scientific) were combined with Laemmli-2-
231 mercaptoethanol (95:5 v/v) sample buffer (1:1 v/v), heated at 80 °C for 10 min, before
232 electrophoresis on Mini-PROTEAN® TGX™ gels at 180 V for 45 min and electro-transfer
233 onto PVDF membrane at 100 V for 45 min. The membrane was blocked in 5% skim milk in
234 Tris buffered saline-Tween 20 (0.1% TBS-Tween) for 1 hour at room temperature with
235 agitation, incubated with the anti-NQO1 antibody (1:200 dilution) in blocking buffer (TBS-
236 Tween milk-5%) overnight at 4°C. Blot was rinsed in TBS-T (1h incubation with replacement
237 of the TBS-Tween buffer by fresh medium every 10 min) and then incubated with the
238 secondary antibody (2 h, room temperature, Goat anti-mouse IgG, 1:2000 dilution in blocking
239 buffer), followed by rinsing. Bands were visualized with enhanced chemiluminescence (ECL)
240 substrate and then imaged using MFChemiBIS 3.2 (DNR Bio-Imaging Systems Ltd.,
241 Jerusalem, Israel). Molecular weight of NQO1 bands was determined by comparison to the
242 Euromedex protein ladder plus prestained (France). The content of soluble NQO1 assemblies
243 was quantified by measuring the intensity of the chemiluminescent bands using GelCapture
244 Software. All samples were analyzed in triplicate.

245

246 *2.2.9. Cytotoxicity tests*

247 4000 cells in 100 µL cell culture medium per well were seeded in 96-well plates and left
248 overnight in the humidified incubator at 37°C with 5% CO_2. On the following day, the
249 treatments, namely free β-Lap (in dimethyl sulfoxide, DMSO), [β-Lap:CD] complexes, β-
250 Lap-loaded nanoparticles, β-Lap-loaded liposomes or [β-Lap:CD] complex-loaded liposomes
251 (in buffer) were added to the cells at different concentrations. Each well contained a final
252 volume of 200 µl of full medium. Final β-Lap concentrations ranged from 0 to 4 µM. Cells
253 were incubated again for 24, 48 or 72 hours in the same conditions. Cell viability was then
254 determined by the MTT test (Labtech LT-5000 Plate Reader). Briefly, 20 µl of 3-(4,5-
255 dimethylthiazol-2-yl)-2,5-diphenyl-2H-tetrazolium bromide were added to each well at the
256 final concentration of 0.5 mg/mL in full medium and incubated at 37°C with 5% CO_2 for 2 h.
257 The medium was then aspirated, taking care not to remove any cell, and the purple formazan
258 product formed was dissolved in 200 µL DMSO. After 10 min shaking, the optical density
259 (OD) at 570 nm of each well was measured using a microplate reader (LT-5000 MS,
260 Labtech). For each plate, each concentration was analyzed in triplicate.

261

262 **3. Results and discussion**

263

264 3.1. Characterization of the interfacial behavior of β-Lap-lipid mixtures

265 Cavalcanti et al. (2011, 2015) prepared β-Lap-loaded liposomes using Epikuron®200
266 (DLOPC), cholesterol and stearylamine. Since DLOPC is highly sensitive to oxidation, we
267 envisaged to replace it by other phospholipids. In a previous work we showed that β-Lap
268 interacts differently with phospholipids, depending on the presence and number of double-
269 bonds. The drug inserts in the lipid bilayer close to the polar head groups in dipalmitoyl

phosphatidylcholine (DPPC), between the polar head groups and double bond in unsaturated palmitoyl-oleoyl-phosphatidylcholine (POPC) or dioleoyl phosphatidylcholine (DOPC) (Wu et al. 2019). POPC could be a good alternative to DLOPC because it is partially saturated. In this work, we compared the interfacial behavior of the two phospholipids alone or mixed with CHOL and SA, in the presence or absence of β-Lap. The results are presented in Figures 2 and 3, and in Tables 1 and 2.

For both drug-lipid mixtures, the π-A isotherms of the mixed β-Lap-lipid monolayers barely differ from those of lipid mixtures without the drug (Figure 2). When looking more closely, a slight change in the shape of the π-A isotherms is observed for monolayers containing DLOPC. This is confirmed by the characteristic values summarized in Table 1. The decrease in the maximal compressibility modulus (C_S^{-1}), although limited, accounts for a disorganization of the monolayers in the presence of β-Lap. Moreover, the compression cycles (Figure 3) show that the profiles of the compression isotherms for POPC and DLOPC monolayers are affected by the presence of β–Lap, especially those of POPC. From the isotherms in Figure 2, free energies of mixing were calculated (Table 2). For both the POPC-CHOL-SA and DLOPC-CHOL-SA mixtures, the ΔG^{exc} values were positive at all surface pressures accounting for an unfavorable interaction between the three components in the two mixtures. ΔG^{mix} values were positive at 30 mN/m, a surface pressure considered to be close to the lateral surface pressure in liposome membranes. The addition of CHOL and SA to the two phospholipids may thus affect the stability of prepared vesicles. Surface pressure measurements also showed that β-Lap tends to disorganize phospholipid-CHOL-SA monolayers. Previous results suggested that CHOL and β-Lap may compete for the same location in vesicles (Wu et al. 2019). As a result, β-Lap could insert less deeply in liposome bilayers than in pure phospholipid vesicles. Aloisio et al. (2017) showed that the encapsulation rate of lipophilic drugs decreases with the cholesterol/phosphatidylcholine (PC)

295 ratio. The presence of cholesterol could thus be detrimental to β-Lap stability in the bilayers
296 and accelerate its release, as reported for vesicles containing paclitaxel and CHOL (Steffes et
297 al. 2017).
298
299
300 **Table 1**. Main characteristics of the π-A isotherms of lipids spread with 3.5 mol% β-Lap onto
301 HEPES buffer at 21°C ± 1°C. A_c: molecular area at collapse; π_c: surface pressure at collapse;
302 $C_s^{-1}{}_{max}$: maximal compressibility modulus.
303

Film forming components	**A_c (Å^2)**	**π_c (mN/m)**	**$C_s^{-1}{}_{max}$ (mN/m)**
Pure POPC	60.0 ± 0.5	44.0 ± 0.2	100.95 ± 3.02
POPC-β-Lap	59.3 ± 1.2	43.5 ± 0.5	101.04 ± 0.39
Pure DLOPC	57.1 ± 0.8	42.8 ± 0.3	104.78 ± 4.40
DLOPC-β-Lap	53.3 ± 1.2	41.6 ± 0.7	95.52 ± 5.08
POPC-CHOL-SA	49.5 ± 0.5	47.8 ± 0.3	169.72 ± 6.02
(POPC-CHOL-SA)-β-Lap	47.0 ± 0.2	47.5 ± 0.0	152.98 ± 4.46
DLOPC-CHOL-SA	50.2 ± 0.8	44.6 ± 0.3	124.23 ± 5.53
(DLOPC-CHOL-SA)-β-Lap	47.8 ± 0.7	43.9 ± 0.6	115.22 ± 5.79

304
305
306 **Table 2:** ΔG^{exc} and ΔG^{mix} values for (a) POPC-CHOL-SA and (b) DLOPC-CHOL-SA mixed
307 monolayers.
308

	POPC-CHOL-SA		DLOPC-CHOL-SA	
Surface pressure (mN/m)	ΔG^{exc} (kJ/mol)	ΔG^{mix} (kJ/mol)	ΔG^{exc} (kJ/mol)	ΔG^{mix} (kJ/mol)
5	0.1773	-0.6282	0.3461	- 0.4594
10	0.3791	-0.4263	0.6851	- 0.1204
15	0.5500	- 0.2554	1.0010	0.1955
20	0.7302	- 0.0752	1.2794	0.4740
25	0.9333	0.1279	1.5453	0.7398
30	1.1860	0.3806	1.8056	1.0002
35	1.3401	0.5346	1.9945	1.1890
40	1.5435	0.7380	2.1243	1.3189
45	1.7443	0.9388	2.2464	1.4409

309

310

311 3.2. Characterization of β-Lap-loaded nanoparticles and liposomes

UV-visible spectroscopy at 256 nm was used to assay β-Lap in nanoparticles and liposomes. Standard calibration curves were obtained with drug concentrations ranging from 5×10^{-6} to 3.5×10^{-5} M in a mixture of methanol and buffer (Figure S1, *in supplementary information*).

The hydrodynamic diameter of PLA nanoparticles was 170 ± 3 nm, with a PDI of 0.08 ± 0.02 and a negative zeta potential value of - 46 ± 1 mV. The encapsulation of β-Lap did not significantly change these characteristics (size: 176 ± 9 nm, PDI: 0.06 ±0.03, ζ-potential: -50 ± 2 mV). Drug EE and ER values were 12.82 and 1.97 % respectively (N'Diaye et al. 2019).

When measuring the absorbance of liposome samples containing SA, the absorption bands of β-Lap appeared always shifted towards lower wavelengths (Figure S2, *in supplementary information*). Since POPC does not display any absorbance peak at wavelengths higher than 203 nm (McHowat et al. 1996), it is possible that β-Lap interacted with SA (Ci et al. 1989). We observed that when β-Lap was encapsulated in liposomes made of POPC only, or solubilized by CDs, its UV-visible absorption spectrum remained unchanged.

In light of these results and those obtained by surface pressure measurements, SA and CHOL were both excluded from liposome composition. Considering the strong sensitivity of DLOPC to oxidation, we encapsulated β-Lap in liposomes made of POPC only. MLVs were prepared, in order to increase the encapsulation rate of the lipophilic drug per vesicle by greater lamellarity. Figure 4 shows the morphology of liposomes and Table 3 summarizes their characteristics. Both extrusion and tip sonication yielded mixtures of mono-, oligo- and multilamellar liposomes.

B-lapachone loaded and unloaded vesicles exhibited monodisperse narrow size distribution characterized by a polydispersity index (PDI) < 0.2 and a mean hydrodynamic diameter around 190 nm (Table 3). Sonicated β-Lap-loaded vesicles appeared smaller than extruded ones, with larger polydispersity index (Figure 4C). The EE values, calculated from direct drug

and phospholipid assays in the vesicle pellets collected after ultracentrifugation, varied between 27 and 34%.

Table 3. Characteristics of unloaded and β-Lap-loaded POPC vesicles. HD: hydrodynamic diameter. E: extrusion. S: tip sonication. Nd: not determined. SD: standard deviation, PDI: polydispersity index.

Composition	Method	HD (nm) (± SD)	PDI (± SD)	ζ-potential (± SD) (mV)	ER (%) (± SD)	EE (%) (± SD)
POPC	E	186.1 ± 20.2	0.083 ± 0.067	nd	-	-
POPC-β-Lap	E	193.4 ± 6.2	0.076 ± 0.005	nd	3.42 ± 0.29	34.2 ± 2.9
POPC-β-Lap	1h-S	167.2 ± 1.2	0.108 ± 0.038	-5.75 ± 0.07	2.90 ± 0.50	29.0 ± 5.0
POPC-β-Lap	0.5h-S	179.9 ± 1.4	0.115 ± 0.016	-2.12 ± 0.13	2.73 ± 0.21	27.3 ±2.1

The presence of β-Lap did not change the morphology of liposome bilayers. This is not surprising considering the small payload of β-Lap in these vesicles and its shallow insertion in lipid bilayers demonstrated by physicochemical and simulation experiments (Wu et al. 2019). For hydrophobic drugs such as β-Lap, the poor loading capacity of liposomes is related to the limited space offered by a lipid bilayer, which leads to low drug-to-lipid ratio (Deo et al. 2004). Excess loading may compromise bilayer integrity, by alteration of the packing of phospholipid molecules. It has been demonstrated that, above a critical saturation concentration, lipophilic drugs such as ibuprofen increase the permeability of the lipid bilayer by formation of transient pores and membrane defects (Angelini et al. 2017). They may even lead to the formation of mixed micelles (Deo et al. 2004). In the case of β-Lap, we did not

observe any apparent instability related to the presence of the drug, although no long-term stability trial was performed.

Increasing the initial drug-to-lipid ratio invariably led to the same final encapsulation rate. For extruded vesicles, drug-to-lipid ratio and ER were equal to 3.54 (± 0.31) and 3.42 mol (± 0.29) %, respectively, and for sonicated vesicles, they were equal to 2.99 and 2.90 mol%, respectively. Compared to the initial drug-to-lipid ratio (10 mol%) in the dried lipid film, there was obviously a significant loss of drug during vesicles preparation. However, the loading rate obtained by sonication or extrusion was very similar to that achieved with other lipophilic drugs. For example, for paclitaxel which is much more lipophilic than β-lapachone, the solubility limit in lipid bilayers was reported to be 3 mol% only (Steffes et al 2017; Bhatt et al. 2018). Aloisio et al. (2017) prepared vesicles by the thin film hydration and dehydration-rehydration methods and compared the encapsulation rate of lipophilic drugs depending on the method used. The thin hydrated film method led to vesicles with only 1 mol% maximal encapsulation rate for pure indomethacin, whereas it was 43 times higher using the dehydration-rehydration method with drug-cyclodextrin complexes entrapped in the aqueous core of vesicles. Obviously, encapsulation of the drug was dramatically enhanced by complexation with cyclodextrins. This is an interesting result because Cavalcanti et al. (2011; 2015) also reported on the encapsulation of [β-Lap:CD] complexes in vesicles. However, they did not study the change in β-Lap ER in these conditions.

3.3. Formation of [β-Lap:CD] complexes

As previously mentioned, a number of researchers have attempted to overcome the low solubility and bioavailability of β-Lap by forming inclusion complexes with cyclodextrins. The association constants were generally determined by the phase solubility method, ^{1}H-

NMR, and fluorescence spectroscopy. Beta-CD and HP-β-CD showed higher binding affinity to β-Lap (K_c = 0.9-1.2 × 10^3 M^{-1}) than α-CD (20 M^{-1}) and γ-CD (160 M^{-1}) (Nasongkla et al. 2003). RM-β-CD and SBE-β-CD both significantly enhanced β-Lap apparent solubility (Cunha-Filho et al. 2007). However, RM-β-CD showed some renal toxicity. Conversely, SBE-β-CD and HP-β-CD appeared well tolerated in humans and did not provoke any significant adverse effects following oral or intravenous administration (Stella and He 2008). Therefore, we chose SBE-β-CD and HP-β-CD and used the drug-to-CD molar ratios already successfully tested by Xavier-Junior et al. (2017) *i.e.*, 1:8 and 1:4 for [β-Lap:HP-β-CD] and [β-Lap:SBE-β-CD] complexes, respectively.

Our solubilization tests indicated that the actual drug-to-CD molar ratios were 1:8.4 (± 0.3) and 1:5.0 (± 0.1) for HP-β-CD and SBE-β-CD, respectively. The obtained solutions of [β-Lap:CD] complexes were filtered and lyophilized. Freeze-drying was necessary to weigh the samples and calculate CD and β-Lap molar ratios. However, after lyophilization of [β-Lap:SBE-β-CD] samples partial separation and crystallization of β-Lap was observed. Apparently, the drug was partially expelled from SBE-β-CD cavities during drying. This separation was not observed for [β-Lap:HP-β-CD] complexes. The interaction of β-Lap with the two cyclodextrin derivatives was analyzed by UV-visible spectroscopy. The absorption spectrum of β-Lap was not modified by complexation with them (Figure S3, *in supplementary information*).

3.4. Formation and characterization of [β-Lap:CD] complexes-loaded liposomes

3.4.1. Formation of double loaded liposomes and determination of the drug loading

Double loaded liposomes are vesicles containing both the drug in their bilayers and [drug:CD] complexes in their aqueous core. During the last two decades, many double loaded liposomes

have been proposed and investigated (Maestrelli et al. 2010; Angelini et al. 2017; Fatouros et al. 2001; Gillet et al. 2009; Gharib et al. 2015; Gharib et al. 2017; Gharib et al. 2018; Zhang et al. 2015a; Zhang et al. 2015b; Zhang et al. 2015c; Soo et al. 2016; Azzi et al. 2018). These systems may allow fast and sustained release. The encapsulation of the [drug:CD] complexes into liposomes combines the advantages offered by both the CDs and the liposomes (Gharib et al. 2015). Liposomes prevent CD complex dissociation due to dilution in the plasma (McCormack and Gregoriadis 1996), and they reduce renal excretion of CD inclusion complexes (Frank et al. 1976). Cyclodextrins increase drug water solubility and, therefore, drug availability. In principle, they can preserve the integrity of the lipid bilayer from the perturbation due to drug insertion in the lipid membrane. However, Ohtani et al. (1989) have shown *in vitro* that certain cyclodextrins can remove some components of human erythrocyte membranes (*e.g.,* phospholipids, cholesterol, and proteins) forming inclusion complexes with them and destabilizing the cell bilayer. For example, HP-β-CD extracts cholesterol from lung epithelial cells (Dos Santos et al. (2017). Also, CDs can participate to the transfer and redistribution of phospholipids in a bilayer, interact with the inner lipid leaflet of the liposomes and transfer their cargo to the bilayer (Zidovetzki and Levitan 2007). Destabilization may follow (Angelini et al. 2017). Methyl-β-cyclodextrin can induce the disruption of vesicles and the formation of micelles (Anderson et al. 2004; Hatzi et al. 2007). At high concentrations, the random methylated β-cyclodextrin adsorbs to dimyristoylphosphatidylcholine vesicles and is able to extract phospholipid molecules (Joset et al. 2015). Many cyclodextrins, including HP-β-CD and SBE-β-CD, alter the permeability of soybean phosphatidylcholine bilayers (Piel et at. 2007). HP-β-cyclodextrin, especially, affects the fluidity and stability of liposomes (Gharib et al. 2018). It interacts with the polar head groups of all phospholipids and with the acyl chains of saturated ones, while disorganizing the unsaturated phospholipids (soybean PC). Considering that POPC has both saturated and

unsaturated chains, the effect of the cyclodextrin could be significant and lead to the release of β-Lap molecules inserted in phospholipid leaflets. The possible interaction of cyclodextrin derivatives with the vesicle bilayer is thus an important point to consider when encapsulating CDs in the aqueous core of liposomes.

In order to better understand the interactions between the three components (*i.e.*, β-Lap, CD and POPC), two protocols were followed: (i) free CDs were added to a POPC film already containing 10 mol% β-Lap and (ii) a solution of [β-Lap : CD] complexes was used to hydrate a POPC film containing 10 mol% β-Lap. The characteristics of the various samples are summarized in Tables 4 and 5.

(i) The first protocol was tried to determine whether the addition of β-CDs to a lipid film containing the drug could allow solubilization and encapsulation of the excess free drug that usually precipitates in the aqueous medium surrounding the vesicles. However, it led to a very low encapsulation rate (0.95 mol%) (Table 4), indicating the extraction of β-Lap from the POPC film without much incorporation of [β-Lap:CD] complexes in the vesicles' core. After ultracentrifugation, most of β-Lap complexed by CD molecules was eliminated with the supernatant. Based on the interaction of β-CD derivatives with phospholipids reported by different research groups (Fatouros et al. 2001; Gharib et al. 2018; Anderson et al. 2004; Hatzi et al. 2007), it is likely that free cyclodextrin molecules interacted with phospholipid ones during film hydration.

Table 4. Characteristics of vesicles formed by hydration of a POPC-β-Lap film by free CDs-containing buffer and tip sonication (S). HD: hydrodynamic diameter. SD: standard deviation.

Cyclodextrin	Lipid film	Method	HD (nm)	PDI	ζ-potential	ER	EE

			(± SD)		(± SD) (mV)	(%)	(%)
SBE-β-CD	POPC +10% β-lapachone	0.5 h-S	169.3 ± 1.7	0.131 ± 0.017	-2.13 ± 0.13	0.95	9.5

449

450 The absorption spectrum of β-Lap showed a blue shift when the POPC-β-Lap film was
451 hydrated with free SBE-β-CDs (Figure S4, *in supplementary information*). This blue shift was
452 not observed for samples in which the drug was already complexed with SBE-β-CD
453 molecules. This modification in the absorption spectrum indicates a change in β-Lap
454 environment that may be attributed to CD-POPC interaction. There are examples of
455 phosphatidylcholines (DPPC, DOPC) solubilized by β-CD and its derivatives, like HP-β-CD
456 (Irie et al. 1992), or methyl-β-CD (Anderson et al. 2004; Hatzi et al. 2007). Anderson et al.
457 (2004) calculated that 2 methyl- β-CD per acyl chain would be necessary to solubilize POPC.
458 We observed a very low encapsulation rate of β-Lap in double loaded vesicles prepared with
459 SBE-β-CD and POPC (Table 4). Complexation of phospholipid molecules would consume
460 more CDs than β-Lap complexation. Because of the high lipid-to-drug ratio, phospholipid
461 might be preferentially complexed by the CDs leading to β-Lap separation.

462 (ii) In the second protocol, [β-Lap:CD] complexes were dissolved in buffer and free β-Lap
463 was solubilized with POPC in the organic phase. There was both excess β-Lap in the dried
464 film, and excess free cyclodextrin cavities in the aqueous medium, because the CD-to-β-Lap
465 ratio necessary for a 1:1 stoichiometry is high (Table 5) (Xavier-Junior et al. 2017).

Table 5. Characteristics of POPC vesicles formed by hydration of a POPC-β-Lap (10 mol%) film by [β-Lap:CD] complexes-containing buffer, at optimal [β-Lap:CD] ratio (1:8.4 and 1:5.0 for HP-β-CD and SBE-β-CD, respectively). Nd: not determined.

[CD:β-Lap] complex	**Method**	**HD (nm) (± SD)**	**PDI**	**ζ-potential (± SD) (mV)**	**ER (%) ± 10%**	**EE (%) ± 10%**
HP-β-CD	E	202.0 ± 5.2	0.099 ± 0.048	Nd	4.30	24.36
SBE-β-CD*	E	159.9 ± 0.8	0.065 ± 0.011	Nd	4.94	27.98
HP-β-CD	1h-S	166.5 ± 1.3	0.113 ± 0.031	-5.63 ± 0.27	4.68	19.43
SBE-β-CD	1h-S	163.4 ± 1.9	0.095 ± 0.027	-5.20 ± 0.26	3.96	21.56
HP-β-CD	0.5h-S	183.6 ± 1.7	0.140 ± 0.016	-1.74 ± 0.16	4.30	21.50
SBE-β-CD	0.5h-S	181.2 ± 1.4	0.122 ± 0.025	-3 .44 ± 0.23	4.72	23.60

*In this sample, the POPC film also contained 2.5% DSPE-PEG_{2000}. A possible explanation for the higher ER observed for this batch could be the enlargement of the aqueous space between bilayers in the presence of PEG chains, allowing the encapsulation of more [β-Lap:CD] complexes.

For all studied systems, mean encapsulation rates (ER) and encapsulation efficiencies (EE) of β-Lap ranged from 3.96% to 4.94% and 19.43% to 27.98%, respectively. These results may be attributed to factors such as the concentration of the phospholipid, the initial drug-to-lipid molar ratio, the preparation methods as well as the presence or not of PEG chains. Higher ER was obtained when β-Lap was solubilized by CDs prior to its encapsulation into liposomes core. This agrees with most published research works on drug-in-cyclodextrin-in-liposomes (Gharib et al. 2015; Gharib et al. 2017; Azzi et al. 2018). The encapsulation efficiency of β-Lap (EE) was lower in the presence of cyclodextrins than in their absence. This has also been frequently reported (Maestrelli et al. 2010; Wang et al. 2016). The increment in encapsulation rate resulting from the addition of [β-Lap:CD] complexes in buffer for thin film rehydration was low relative to the excess free β-Lap in the medium. This demonstrates the non-proportionality between the initial β-Lap amount (in the lipid film and complexed with CDs) and the amount of successfully encapsulated drug.

3.4.2. Morphology of the double loaded vesicles

The morphology of [β-Lap:CD]-liposomes was analyzed by cryoTEM. Mixtures of uni-, and oligo-lamellar vesicles were obtained by both extrusion (Figure 5A,B) and sonication (Figure 5C). Lamellarity slightly decreased for the extruded vesicles. Again, sonication yielded more polydisperse vesicles than extrusion, as deduced from DLS measurements.

3.4.3. Biological efficiency of the various formulated systems

We studied the effect of β-Lap free in the medium, solubilized in β-cyclodextrin derivatives or encapsulated in vesicles or nanoparticles, on the viability of different cells lines. The first objective was to test the toxicity of β-Lap against cells of different origins, but also on cancer

500 and normal cells that can coexist in a same tissue. The second objective was to evaluate the
501 NQO1-dependent cytotoxicity of β-lapachone in prostate cancer suggested in the literature
502 (Planchon et al 2001; Li et al 2003). If it is well known that PC-3 is NQO1-positive (Thapa et
503 al. 2014) and NIH 3T3 NQO1-negative (Powis et al. 1995), the level of expression of NQO1
504 in PNT2 cells was unknown. We first verified NQO1 expression in both PC-3 and PTN2
505 (Figure 6). The bands located between 28 and 36 kDa correspond to the molecular weight of
506 NQO1 (31 kDa). Both prostate cell lines are thus NQO1+.

507 Cytotoxicity of free β-Lap at 24, 48 and 72 h following addition of the drug in the cell culture
508 medium was evaluated in the three cell lines. For NIH 3T3 cells, the half maximal inhibitory
509 concentration (IC_{50}) decreased from 2.9 to 1.6 and then 0.7 µM after 24 h, 48h and 72 h of
510 contact with cells, respectively (Figure 7). NIH 3T3 cells grow very fast, which could explain
511 their high sensitivity to the treatment. However, cells seemed resistant to β-Lap above 4 µM.
512 For PNT2, IC_{50} values ranged between 2.2 and 1 µM depending on the incubation time, and
513 for PC-3 cells, the obtained IC_{50}values were very similar (2.4 to 1.2 µM) (Figure 7).

514 According to Li et al. (2003), normal cells are more resistant to β-Lap than tumor cells. This
515 is true for NIH 3T3 cells but only at high β-Lap concentrations. The cytotoxicity of β-Lap
516 against epithelial and cancer cells was almost identical, which calls into question the
517 selectivity of the β-Lap treatment. As previously mentioned, both PC-3 and PNT2 cells are
518 NQO1+. Conversely, NIH 3T3 cells are NQO1 negative but were also affected by β-Lap,
519 although they were less sensitive at high concentrations. This means that drug toxicity against
520 any of these cells could be controlled by another mechanism of action of β-Lap than NQO1-
521 mediated apoptosis, like cell cycle arrest or targeting of other proteins (Kung et al. 2008). The
522 mechanism of β-lapachone cytotoxicity is more complex than previously stated.

Further reported results correspond to cell viability after 48h incubation with the drug, excipients or drug carriers (Table 6 and Figure 8). The cytotoxicity of β-Lap-loaded nanoparticles against PNT2 was not studied, considering the non-negligible cytotoxicity of PLA nanoparticles in contact with these cells (Table 6). All IC_{50} values for PNT2 cells were lower than those for PC-3 ones confirming that immortalized epithelial prostate cells were slightly more sensitive to β-Lap than cancer cells. However, Figure 8 (A,B) shows some resistance of PNT2 cells to the treatment above 1 µM. This is not the case for PC-3 cells (Figure 8 (C,D)) for which a dose-response profile was observed with all treatments.

Table 6: IC_{50} values at 48h for β-Lap free or inserted in various drug delivery systems. Standard deviations did not exceed 10%. Nd: not determined

System	β-Lap	PNT2, IC_{50} (µM)	PC-3, IC_{50} (µM)
POPC vesicles	-	500	>1000
PLA NPs	-	150 (µg/mL)	> 2200 (µg/mL)
HP-β-CD	-	7000	>10000
SBE-β-CD	-	2000	1800
Free β-Lap	DMSO	1.0	1.6
[HP-β-CD: β-Lap]	complexed	1.0	1.7
[SBE-β-CD: β-Lap]	complexed	1.0	1.8
β-Lap-loaded NPs	encapsulated	Nd	1.3

β-Lap-loaded vesicles	inserted in bilayers	1.7	3.6
Liposome/HP-β-CD/ β-Lap	Double loaded	0.6	1.9
Liposome/SBE-β-CD/ β-Lap	Double loaded	0.9	2.2

534

535 As expected from the previous work of Nasongkla and coworkers (2003), toxicity of the pure
536 cyclodextrin derivatives was observed at much higher concentrations than those necessary to
537 solubilize β-Lap (Table 6). SBE-β-CD affected more the cell viability than HP-β-CD, and
538 IC_{50} of both cyclodextrin derivatives were lower for PNT2 cells than for PC3 ones. However,
539 cell viability profiles of β-Lap in CD complexes were similar to those of free β-Lap
540 solubilized in DMSO, which confirms the poor cytotoxicity of cyclodextrins in the conditions
541 used (Figure 8 (A,C), Table 6).

542 Many authors have reported the enhancement of the cytotoxicity of a drug when complexed
543 with cyclodextrins. This was the case for telmisartan, niclosamide and paclitaxel in HP-β-CD
544 complexes (Kaur et al. 2014, Lodagekar et al. 2019, Shen et al. 2020) or chrysin in SBE-β-CD
545 ones (Kulkarni and Belgamwar 2017). However, this enhanced cytototoxicity seemed merely
546 related to the better solubilization of the drugs in cyclodextrins than in the buffer used for
547 experiments.

548 In our system, cyclodextrins did not add to β-Lap toxicity, probably because the free β-Lap
549 was already solubilized in DMSO prior to addition to the cell culture medium. In their
550 experiments, Nasongkla et al. (2003) also observed that the toxic dose killing 50% of MCF-7
551 cells after 4h contact was similar when β-Lap was solubilized in HP-β-CD (2.1 µM) or in

552 DMSO (1.7 µM). If β-Lap had been dispersed in buffer, the results would certainly have been
553 different.

554 Cyclodextrins contributed to β-Lap solubilization but had no apparent effect on drug
555 permeability nor drug activity. Liossi et al. (2017) who studied by differential scanning
556 calorimetry measurements the interaction of [irbesartan:HP-β-CD] complexes with
557 dipalmitoylphosphatidylcholine vesicles showed that HP-β-CD adsorbed at the surface of
558 phospholipid bilayers and contributed to the solubilization of the drug in the bilayer. Indeed,
559 when irbesartan was free, crystals formed in the membrane, suggesting that the drug
560 aggregated. In our system, β-Lap would not aggregate in the membrane at concentration
561 below 4 mol% (Wu et al. 2019). In fact, it is reasonable to think that it would be released from
562 cyclodextrin complexes near the cell membrane, which would explain the similar viability
563 profiles observed in the presence and absence of cyclodextrins. Other authors reported a lower
564 or similar cytotoxicity of [drug:cyclodextrin complexes], compared to free drug. This was the
565 case for campthotecine, zerumbone, chlorzoxazone, barbigerone or budesonide complexed
566 with HP-β-CD (Sætern et al. 2004; Eid et al. 2011; Tang et al. 2015; Qiu et al. 2015; Dos
567 Santos et al. 2017).

568 The cytotoxicity of β-Lap-loaded liposomes against PNT2 cells also appeared similar to that
569 of β-Lap solubilized in DMSO (IC_{50} = 1.7 and 1.0 µM, respectively), but it was lower than the
570 free drug against PC-3 cells (3.6 versus 1.6 µM). A resistance to the treatment was observed
571 for all studied liposome formulations in contact with PNT2 cells at concentrations exceeding
572 the IC_{50} (Figure 8B). Conversely for PC-3 cells (Figure 8 C,D), typical dose-response
573 relationships were obtained, and the cytotoxicity of the formulated systems can be ranked in
574 the following manner: β-Lap-loaded nanoparticles ≥ [CD: β-Lap] complexes ≥ double loaded
575 vesicles > β-Lap-loaded vesicles. The difference between the three first systems may be

576 considered as insignificant. Although the cytotoxicity of all formulated systems was not very
577 different from that of the free β-Lap, they allowed drug solubilization, which is mandatory for
578 its injection. When considering the ER values, the [β-Lap:CD] complexes and double loaded
579 vesicles seem the most efficient systems for β-Lap treatment of prostate cancer.

580 The sensitivity of NIH 3T3 and PNT2 cells to β-Lap at low concentration however highlights
581 the necessity to target β-Lap towards cancer cells. Since NQO1-controlled targeting does not
582 seem effective, functionalized double-loaded liposomes could, in the end, be more interesting
583 systems than simple CDs, especially when considering the methemoglobinemia/hemolytic
584 side-effects observed with the [β-Lap:HP-β-cyclodextrin] complex used in clinical trials.

585

586 **4. Conclusion**

587 This study was aimed at evaluating the effect β-lapachone in different formulated systems for
588 the treatment of prostate cancer. Nanoparticles, cyclodextrins and liposomes allowed
589 solubilizing β-Lap. Various parameters of the encapsulation of β-Lap and [CD:drug]
590 complexes in liposomes were compared, namely morphology, encapsulation rate (ER),
591 encapsulation efficiency (EE), and *in vitro* cytotoxicity on PC-3, PNT2 and NIH 3T3 cells.
592 ER and EE values were particularly low for nanoparticles. In agreement with most studies
593 published on double loaded liposomes, the [drug:CD] complexes allowed reaching higher
594 encapsulation rates but with lower encapsulation efficiency than β-Lap-loaded vesicles.
595 Double loading is costly, as more β-Lap is wasted during liposome preparation. The study of
596 the interaction between β-lapachone, the CDs and POPC showed that CDs interacted with
597 both the drug and phospholipid, and this affected the EE and ER values. Viability tests and
598 EE and ER values led to the conclusion that CDs, and to a smaller extent the double loaded
599 vesicles, were more efficient drug delivery systems than liposomes. However, viability tests

also highlighted the non-negligible sensitivity of PNT2 and NIH 3T3 cells to the drug. The similar cytotoxicity of β-Lap against NQO1-positive and NQO1-negative cell lines calls into question the NQO1-related selectivity of β-Lap in cancer suggested by some authors. Obviously, β-Lap activity does not solely depend on NQO1 expression and NQO1-induced apoptosis pathways. If β-Lap is not selective then it must be targeted. Ligand-functionalized double loaded liposomes could prove interesting systems for this purpose.

Acknowledgements

The authors are thankful to Dr Sylvain Trépout (Institut Curie, Orsay, France) for assistance in cryoTEM experiments, Ms Stéphanie Denis (Institut Galien Paris Saclay, Châtenay-Malabry, France) for training in cell culture, and to Prof. Nereide Stela Santos-Magalhães (Immunopathology Laboratory Keizo Asami, Federal University of Pernambuco, Recife, Brazil) and Dr François-Xavier Legrand (Institut Galien Paris Saclay, Châtenay-Malabry, France) for helpful discussions.

Funding

The PhD thesis of XW was funded by the China Scholarship Council (CSC).

References

Abreu C.A., Ferreira D.C.M., Wadhawan J., Amatore C., Ferreira V.F., da Silva M.N., de Souza M.C.B.V., Gomes T.S., Ximenes E.A., Goulart M.O.F., Electrochemistry of β-lapachone and its diazoderivative: Relevance to their compared antimicrobial activities,

622 *Electrochem. Commun.* **2005**, 7, 767–772. doi:10.1016/j.elecom.2005.04.029

623 Aloisio C., Antimisiaris S.G., Longhi M.R., Liposomes containing cyclodextrins or
624 meglumine to solubilize and improve the bioavailsability of poorly soluble drugs, *J. Molec.*
625 *Liquids*, **2017**, *229*, 106-113. doi: 10.1016/j.molliq.2016.12.035

626 Anderson T.G., Tan A., Ganz P., Seelig J., Calorimetric measurement of phospholipid
627 interaction with methyl-β-cyclodextrin, *Biochemistry* **2004**, *43*, 2251-2261.
628 doi:10.1021/bi0358869

629 Angelini G., Campestre C., Boncompagni S., Gasbarri C., Liposomes entrapping β-
630 cyclodextrin/ibuprofen inclusion complex: Role of the host and the guest on the bilayer
631 integrity and microviscosity, *Chem. Phys. Lipids* **2017**, *209*, 61-65. doi:
632 10.1016/j.chemphyslip.2017.09.004

633 Azzi J., Auezova L., Danjou P.-E., Fourmentin S., Greige-Gerges H., First evaluation of drug-
634 in-cyclodextrin-in-liposomes for an encapsulating system for nerolidol, *Food Chem*. **2018**,
635 *255*, 399-404. Doi: 10.1016/j.foodchem.2018.02.055

636 Bangham A.D., Standish M.M., Watkins J.C., Diffusion of univalent ions across the lamellae
637 of swollen phospholipids, *J. Mol. Biol*. **1965**, *13*, 238-252.

638 Bhatt P., Lalani R., Vhora I., patil S., Amrutiya J., Misra A., Mashru R., Liposomes
639 encapsulating native and cyclodextrin enclosed paclitaxel: enhanced loading efficiency and
640 its pharmacokinetic evaluation, *Int. J. Pharm*. **2018**, *536*, 95-107.

641 Blanco E., Bey1 E.A., Dong Y., Weinberg B.D., Sutton D.M., Boothman D.A., Gao J., -
642 containing PEG-PLA polymer micelles as novel nanotherapeutics against NQO1-
643 overexpressing tumor cells, *J. Control Release* **2007**, *122*, 365-374.
644 doi:10.1016/j.jconrel.2007.04.014

645 Cavalcanti I.M.F., Mendonça E.A.M., Lira M.C.B., Honrato S.B., Camara C.A., Amorim
646 R.V.S., Filho J.M., Rabello M.M, Hernades M.Z., Ayala A.P., Santos-Magalhaes, The
647 encapsulation of β-lapachone in 2-hydroxypropyl-β-cyclodextrin inclusion complex into
648 liposomes: A physicochemical evaluation and molecular modeling approach, *Eur. J.*
649 *Pharm. Sci.,* **2011**, *44*, 332-340.

650 Cavalcanti I.M.F., Pontes-Neto J.G., Kocerginsky P.O., Bezerra-Neto A.M., Lima J.L.C.,
651 Lira-Nogueira M.C.B., Maciel M.A.V., Neves R.P., Pimentel M.F., Santos-Magalhaes
652 N.S., Antimicrobial activity of β-lapachone encapsulated into liposomes against
653 methicillin-resistant *Staphylococcus aureus* and *Cryptococcus neoformans* clinical strains,
654 *J. Global Antimicrob. Resist.* **2015**, *3*, 103-108. doi: 10.1016/j.jgar.2015.03.007

655 Chen Jr P.S., Toribara T.Y., Warner H. Microdetermination of phosphorus, *Anal.*
656 *Chem.* **1956**, *28*, 1756-1758. doi: 10.1021/ac60119a033

657 Ci X., Silva R.S., Nicodem D., Whitten D.G., Electron and hydrogen atom transfer
658 mechanisms for the photoreduction of O-quinones Visible-light induced photoreactions of
659 beta-lapachone with amines, alcohols and amino alcohols, *J. Am. Chem. Soc.* **1989**, *111*,
660 1337-1343. doi: 10.1021/ja00186a029

661 Cunha-Filho M.S.S., Dacunha-Marinho B., Torres-Labandeira J.J., Martínez-Pacheco R.,
662 Landin M., Characterization of β-lapachone and methylated β-cyclodextrin solid-state
663 system, *AAPS PharmSciTech* **2007**, *8*, Article 60.

664 Cunha-Filho M.S.S., Martínez-Pacheco R., Landin M., Effect of storage conditions on the
665 stability of β-lapachone in solid state and in solution: β-lapachone stability studies, *J.*
666 *Pharm. Pharmacol.* **2013**, *65*, 798–806. doi: 10.1111/jphp.12040

667 Deo N., Somasundaran T., Somasundaran P., Solution properties of amitriptyline and its
668 partitioning into lipid bilayers, *Colloids Surf. B: Biointerfaces* **2004**, *34*, 155-159.
669 doi:10.1016/j.colsurfb.2003.10.019

670 Dos Santos A.G., Bayiha J.C., Dufour G., Cataldo D., Evrard B., Silva L.C., Deleu M.,
671 Mingeot-Leclercq M.-P., Changes in membrane biophysical properties induced by the
672 Budesonide/ hydroxypropyl-β-cyclodextrin complex, *Biochim. Biophys. Acta* **2017**, *1859*,
673 1930-1940. Doi: 10.1016/j.bbamem.2017.06.010

674 Eid E.E.M., Abdul A.B., Suliman F.E.O., Sukari M.A., Rasedee A., Fatah S.S.,
675 Characterization of the inclusion complex of zerumbone with hydroxypropyl-β-
676 cyclodextrin, Carbohydrate Polym. 2011, 83, 1707-1714. Doi:
677 10.1016/j.carbpol.2010.10.033

678 Fatouros D.G., Hatzidimitriou K., Antimisiaris S.G., Liposomes encapsulating prednisolone
679 and prednisolone-cyclodextrin complexes: comparison of membrane integrity and drug
680 release, *Eur. J. Pharm. Sci.* **2001**, *13*, 287-296.

681 Frank D.W., Gray J.E., Weaver R.N., Cyclodextrin nephrosis in the rat, *Am. J. Pathol.*, **1976**,
682 *83*, 367-382.

683 Gillet A., Grammenos A., Compère P., Evrard B., Piel G., Development of a new topical
684 system drug-in-cyclodextrin-in-deformable liposome, *Intern. J. Pharm.* **2009**, *380*, 174-
685 180. doi:10.1016/j.ijpharm.2009.06.027

686 Gharib R., Greige-Gerges H., Fourmentin S., Charcosset C., Auezova L., Liposomes
687 incorporated cyclodextrin-drug inclusion complexes: Current state of knowledge,
688 *Carbohydr. Polym.* **2015**, *129*, 175-186. doi: 10.1016/j.carbpol.2015.04.048

689 Gharib R., Auezova L., Charcosset C., Greige-Gerges H., Drug-in-cyclodextrin-in-liposomes
690 as a carrier system for volatile essential oil components: Application to anethole, *Food*
691 *Chem.,* **2017**, *218*, 365-371. doi: 10.1016/j.foodchem.2016.09.110

692 Gharib R., Fourmentin S., Charcosset C., Greige-Gerges H., Effect of hydroxypropyl-β-
693 cyclodextrin on lipid membrane fluidity, stability and freeze-drying of liposomes, *J. Drug*
694 *Deliv. Sci. Technol.* **2018**, *44*, 101-107. Doi: 10.1016/j.jddst.2017.12.009

695 Hartner L.P., Rosen L., Hensley M., Mendelson D., Staddon A.P., Show W., Kovalyov O.,
696 Ruka W., Skladowski K., Jagiello-Gruszfeld A., Byakhov M., Phase 2 dose multi-center,
697 open-label study of ARQ 501, a checkpoint activator, in adult patients with persistent,
698 recurrent or metastatic leiomyosarcoma (LMS), J. Clin. Oncol. 2007, 25, 20521. Doi:
699 10.1200/jco.2007.25.18_suppl.20521.

700 Hatzi P., Mourtas S., Klepetsanis P.G., Antimisiaris S.G., Integrity of liposomes in presence
701 of cyclodextrins: Effect of liposome type and lipid composition, *Intern. J. Pharm*, **2007**,
702 *333*, 167-176. Doi: 10.1016/j.ijpharm.2006.09.059

703 Irie T, Fukunaga K., Pitha J., Hydroxypropylcyclodextrins in parenteral use. I: Lipid
704 dissolution and effects on lipid transfers in vitro. *J. Pharm. Sci.* **1992**, *81*, 521–523.

705 Joset A., Grammenos A., Hoebeke M., Leyh B., Investigation of the interaction between a β-
706 cyclodextrin and DMPC liposomes: a small angle neutron scattering study, *J. Incl.*
707 *Phenom. Macrocycl. Chem.* **2015**, *83*, 227-238. Doi: 10.1007/s10847-015-0558-z

708 Kaur M., Bhatia R.K., Pissurlenkar R.R.S., Coutinho E.C., Jain U.K., Katare O.P., Chandra
709 R., Madan J., Telmisartan complex augments solubility, dissolution and drug delivery in
710 prostate cancer cells, *Carbohydrate Polym.* **2014**, *101*, 614-622. Doi:
711 10.1016/j.carbpol.2013.09.077

712 Kulkarni A.D., Belgamwar V.S., Inclusion complex of chrysin with sulfobutyl ether-β-
713 cyclodextrin (Captisol®): Preparation, characterization, molecular modelling and in vitro
714 anticancer activity, J. *Molec. Struct.* **2017**, *1128*, 563-571. Doi:
715 10.1016/j.molstruc.2016.09.025

716 Kumi-Diaka J., Chemosensitivity of human prostate cancer cells PC-3 and LNCaP to
717 genistein isoflavone and β-lapachone, *Biol. Cell* **2002**, *94*, 37-44.

718 Kung H.-N., Yang M.-J., Chang C.-F., Chau Y.-P., Lu K.-S., *In vitro* and *in vivo* wound
719 healing-promoting activities of β-lapachone, *Am. J. Physiol. Cell Physiol*. **2008**, *295*,
720 C931-943.

721 Lamberti M.J., Vittar N.B.R., de Carvalho da Silva F., Ferreira V.F., Rivarola V.A.
722 Synergistic enhancement of antitumor effect of β-lapachone by photodynamic induction of
723 quinone oxidoreductase (NQO1), *Phytomedicine*, **2013**, *20*, 1007-1012. Doi:
724 10.1016/j.phymed.2013.04.018

725 Lee H.J., Cheong J., Park Y.M., Choi Y.H., Down-regulation of cyclooxygenase-2 and
726 telomerase activity by β-lapachone in human prostate carcinoma cells, *Pharmacol. Res*.
727 **2005**, *51*, 553-560. doi:10.1016/j.phrs.2005.02.004

728 Li Y., Sun X., LaMont J.T., Pardee A.B., Li C.J., Selective killing of cancer cells by β-
729 lapachone: Direct checkpoint activation as a strategy against cancer, *PNAS*, **2003**, *100*,
730 2674-2678. doi: 10.1073/pnas.0538044100

731 Liossi A.S., Ntountaniotis D., Kellici T.F., Chatziathanasiadou M.V., Megariotis G., Mania
732 M., Becker-Baldus J., Kriechbaum M., Krajnc A., Christodoulou E., Glaubitz C., Rappolt
733 M., Amenitsch H., Mali G., Theodorou D.N., Valsami G., Pitsikalis M. Iatrou H., Tzakos
734 A.G., Mavromoustakos T., Exploring the interactions of irbersartan and irbesartan-2-

735 hydroxypropyl-β-cyclodextrin complex with model membranes, *Biochim. Biophys. Acta*
736 **2017**, *1859*, 1089-1098. Doi: 10.1016/j.bbamem.2017.03.003

737 Lodagekar A., Borkar R.M., Thatikonda S., Chavan R.B., Naidu V.G.M., Shastri N.R.,
738 Srinivas R., Chella N., Formulation and evaluation of cyclodextrin complexes for
739 improved anticancer activity of repurposed drug: Niclosamide, *Carbohydrate Polym.* **2019**,
740 *212*, 252-259. Doi: 10.1016/j.carbpol.2019.02.041

741 Ma J., Lim C., Sacher J.R., Van Houten B., Qian W., Wipf P., Mitochondrial targeted β-
742 lapachone induces mitochondrial dysfunction and catastrophic vacuoliezation in cancer
743 cells, *Bioorg. Med. Chem. Lett*. **2015**, *25*, 4828–4833. doi: 10.1016/j.bmcl.2015.06.073

744 Maestrelli F., Gonzalez-Rodriguez M.L., Rabasco A.M., Ghelardini C., Mura P., New "drug-
745 in cyclodextrin-in deformable liposomes" formulations to improve the therapeutic efficacy
746 of local anesthetics, *Intern. J. Pharm.*, **2010**, *395*, 222-231. doi:
747 10.1016/j.ijpharm.2010.05.046

748 Mangas-Sanjuan V., Gutierrrez-Nieto J., Echezarreta-Lopez M., Gonzalez-Alvarez I.,
749 Gonzalez-Alvares M., Casabo V.-G., Bermejo M., Landin M., Intestinal permeability of β-
750 lapachone and its cyclodextrin complexes and physical mixtures, *Eur. J. Drug Metab.*
751 *Pharmacokinet.* **2016**, *41*, 795-806. doi: 10.1007/s13318-015-0310-5

752 McHowat J., Jones J. H., Greer M. H., Quantitation of individual phospholipid molecular
753 species by UV absorption measurements, *J. Lipid Res.*, **1996**, *37*, 2450-2460.

754 McCormack B., Gregoriadis G., Comparative studies of the fate of free and liposome-
755 entrapped hydroxypropyl-/3-cyclodextrin/drug complexes after intravenous injection into
756 rats: implications in drug delivery, *Biochimica et Biophysica Acta*, **1996**, *1291*, 237-244

757 Moreno E., Schwartz J., Larrea E., Conde I., Font M., Sanmartin C., Irache J.M., Espuelas S.,

758 Assessment of β-lapachone loaded in lectithin—chitosan nanoparticles for the topical
759 treatment of cutaneous leishmaniasis in *L. major* infected BALB/c mice, *Nanomedicine:*
760 *NBM,* **2015**, *11*, 2003–2012. doi: 10.1016/j.nano.2015.07.011

761 N'Diaye M., Vergnaud-Gauduchon J., Nicolas V., Faure V., Denis S., Abreu S., Chaminade
762 P., Rosilio V., Hybrid lipid polymer nanoparticles for combined chemo- and photodynamic
763 therapy, *Mol. Pharmaceutics* **2019**, *16*, 4045-4058. Doi:
764 10.1021/acs.molpharmaceut.9b00797

765 Nasongkla N., Wiedmann A.F., Bruening A., Beman M., Ray D., Bornmann W.G., Boothman
766 D.A., Gao J., Enhancement of solubility and bioavailability of using cyclodextrin inclusion
767 complexes, *Pharm. Res.* **2003**, *20*, 1626–1633.

768 Ohtani Y., Irie T., Uekama K., Fukunaga K., Pitha J., Differential effects of alpha-, beta- and
769 gamma-cyclodextrins on human erythrocytes, *Eur. J. Biochem*. **1989**,186(1-2), 17-22

770 Piel G., Piette M., Barillaro V., Castagne D., Evrard B., Delattre L., Study of the interaction
771 between cyclodextrins and liposome membranes: effect on the permeability of liposomes,
772 *J. Incl. Phenom. Macrocycl. Chem.* **2007**, *57*, 309-311. doi: 10.1007/s10847-006-9178-y

773 Planchon S.M., Pink J.J., Tagliarino C., Bornmann W.G., Varnes M.E., Boothman D.A., β-
774 lapachone-induced apoptosis in human prostate cancer cells: involvement of NQO1/xip3,
775 *Exp. Cell Res.* **2001**, *267*, 95-106. doi: 10.1006/excr.2001.5234

776 Powis G., Gasdaska PY, Gallegos A, Sherrill K, Goodman D., Over-expression of DT-
777 diaphorase in transfected NIH 3T3 cells does not lead to increased anticancer quinone drug
778 sensitivity: a questionable role for the enzyme as a target for bioreductively activated
779 anticancer drug, *Anticancer Res.*, **1995**, *15*, 1141-1145.

780 Qiu N., Cai L., Wang W., Wang G., Cheng X., Xu Q., Wen J., Liu J., Barbigerone-in-
781 hydroxypropyl-β-cyclodextrin-liposomal nanoparticle: preparation, characterization and
782 anti-cancer activity, *J. Inc. Phenom. Macrocl. Chem.* **2015**, *82*, 505-514. Doi:
783 10.1007/s10847-015-0533-8

784 Roseanu A., Florian P.E., Moisei M., Sima L.E., Evans R.W., Trif M. Liposomalization of
785 lactoferrin enhanced its anti-tumoral effects on melanoma cells, *Biometals,* **2010**, *23*, 485-
786 492. Doi: 10.1007/s10534-010-9312-6

787 Sætern A., Brandl M., Bakkelund W., Sveinbjørnsson, Cytotoxic effect of different
788 camptothecin formulations on human colon carcinoma *in vitro*, *Anti-Cancer Drugs* **2004**,
789 *15*, 899-906. Doi: 10.1097/00001813-200410000-00011.

790 Soo E., Thakur S., Qu Z., Jambhrunkar S., Parekh H.S., Popat A., Enhancing delivery and
791 cytotoxicity of resveratrol through a dual nanoencapsulation approach, *J. Colloid Interface*
792 *Sci.* **2016**, 462, 368-374. Doi: 10.1016/j.jcis.2015.10.022

793 Steffes V.M., Murali M.M., Park Y., Fletcher B.J., Ewert K.K., Safinya C.R., Distinct
794 solubility and cytotoxicity regimes of paclitaxel-loaded cationic liposomes at low and high
795 drug content revealed by kinetic phase behavior and cancer cell viability studies,
796 *Biomaterials*, **2017**, *145*, 242-255. doi: 10.1016/j.biomaterials.2017.08.026

797 Stella V.J., He Q., Cyclodextrins, *Toxicol. Pathol*. **2008**, *36*, 30-42.

798 Tang P., Li S., Wang L., Yang H., Yan H., Li H., Inclusion complexes of chlorzoxazone with
799 β- and hydroxypropyl-β-cyclodextrin: Characterization, dissolution, and cytotoxicity,
800 Carbohydrate Polym. 2015, 131, 297-305. Doi: 10.1016/j.carbpol.2015.05.055

801 Thapa D., Meng P., Bedolla R.G., Reddick R.L., Kumar A.P., Ghosh R., NQO1 suppresses
802 NF-kB-p300 interaction regulate inflammatory mediators associated with prostate
803 tumorigenesis, *Cancer Res.*, **2014**, *74*, 5644-5655. doi: 10.1158:0008-5472.CAN-14-0562

804 Tseng C.-H., Cheng C.-M., Tzeng C.-C., Peng S.-I., Yang C.L., Synthesis and anti-
805 inflammatory evaluations of β-lapachone derivatives, *Bioorg. Med. Chem.* **2013**, *21,* 523–
806 531. doi: 10.1016/j.bmc.2012.10.047

807 Wang W.-X., Feng S.-S., Zheng C.-H., A comparison between conventional liposome and
808 drug-cyclodextrin complex in liposome system, *Intern. J. Pharm.* **2016**, *513*, 387-392. Doi:
809 10.1016/j.ijpharm.2016.09.043

810 Wu X., Chantemargue B., Di Meo F., Bourgaux C., Chapron D., Trouillas P., Rosilio V.,
811 Deciphering the peculiar behavior of β-lapachone in lipid monolayers and bilayers,
812 *Langmuir* **2019**, *35*, 14603–14615. doi: 10.1021/acs.langmuir.9b02886

813 Xavier-Junior F.H., Rabello M.M., Hernandes M.Z., Dias M.E.S., Andrada O.H.M.S.,
814 Bezerra B.P., Ayala A.P., Santos-Magalhaes N.S., Supramolecular interactions between β-
815 lapachone with cyclodextrins studied using isothermal titration calorimetry and molecular
816 modeling, *J. Mol. Recognit.* **2017**, e2646. doi: 10.1002/jmr.2646

817 Zhang L., Tatsuno T., Hasegawa I., Tadano T., Ohta T., Furanonaphthoquinones from
818 Tabebuia avellanedae induce cell cycle arrest and apotosis in the human non-cell lung
819 cancer cell line A549, *Phytochemistry Lett.* **2015a**, *11*, 9-17. doi:
820 10.1016/j.phytol.2014.09.013

821 Zhang L., Zhang Q., Wang X., Zhang W., Lin C., Chen F., Yang X., Pan W., Drug-in-
822 cyclodextrin-in-liposomes: A novel drug delivery system for flurbiprofen, *Intern. J.*
823 *Pharm.* **2015b**, *492*, 40-45. doi: 10.1016/j.ijpharm.2015.07.011

824 Zhang W., Wang G., Falconer J.R., Baguley B.C., Shaw J.P., Liu J., Xu H., See E., Sun J., Aa
825 J., Wu Z., Strategies to maximize liposomal drug loading for a poorly water-soluble
826 anticancer drug, *Pharm. Res*. **2015c**, *32* ,1451-1461.

827 Zidovetzki R., Levitan I., Use of cyclodextrins to manipulate plasma membrane cholesterol
828 content: evidence, misconceptions and control strategies, *Biochim. Biophys. Acta*, **2007**,
829 *1768*, 1311-1324. doi: 10.1016/j.bbamem.2007.03.026

Legends to the figures

Figure 1: Chemical structures of (A) β-Lapachone; (B) PLA; (C) Cholesterol; (D) POPC, (E) DLOPC; (F) Stearylamine; (G) HP and SBE-β-Cyclodextrins.

Figure 2: Mean π-A isotherms and C_s^{-1}-π relationships for monolayers of DLOPC (A,C), POPC (B,D) and their mixtures with CHOL and SA spread on HEPES buffer in the absence or presence of 3.5 mol% β-Lap.

Figure 3: Compression cycles for (A) DLOPC, (B) POPC mixed monolayers with CHOL and SA, in the absence or presence of β-Lap.

Figure 4. Cryo-TEM micrographs of unloaded (A) and β-lapachone-loaded (B,) POPC vesicles prepared by extrusion; (C) β-lapachone-loaded POPC vesicles prepared by tip sonication.

Figure 5. Cryo-TEM micrographs of liposomes obtained from a film of POPC-β-Lap hydrated by (A) [β-Lap:HP-β-CD] and (B,C) [β-Lap:SBE-β-CD] complexes. (A) and (B) were prepared by extrusion and (C) by tip sonication.

Figure 6: Western blot for NQO1 expression in PC-3 and PNT2 cells (n = 3).

Figure 7: Effect of free β-Lap on the viability of (A) mouse fibroblasts, (B) PNT2 and (C) PC-3 cells.

Figure 8. Cytotoxic effect of free β-Lap, β-Lap loaded vesicles, inclusion complexes and double loaded vesicles on (A, B) PNT2 and (C, D) PC-3 cells after 48 h contact, relative to control.

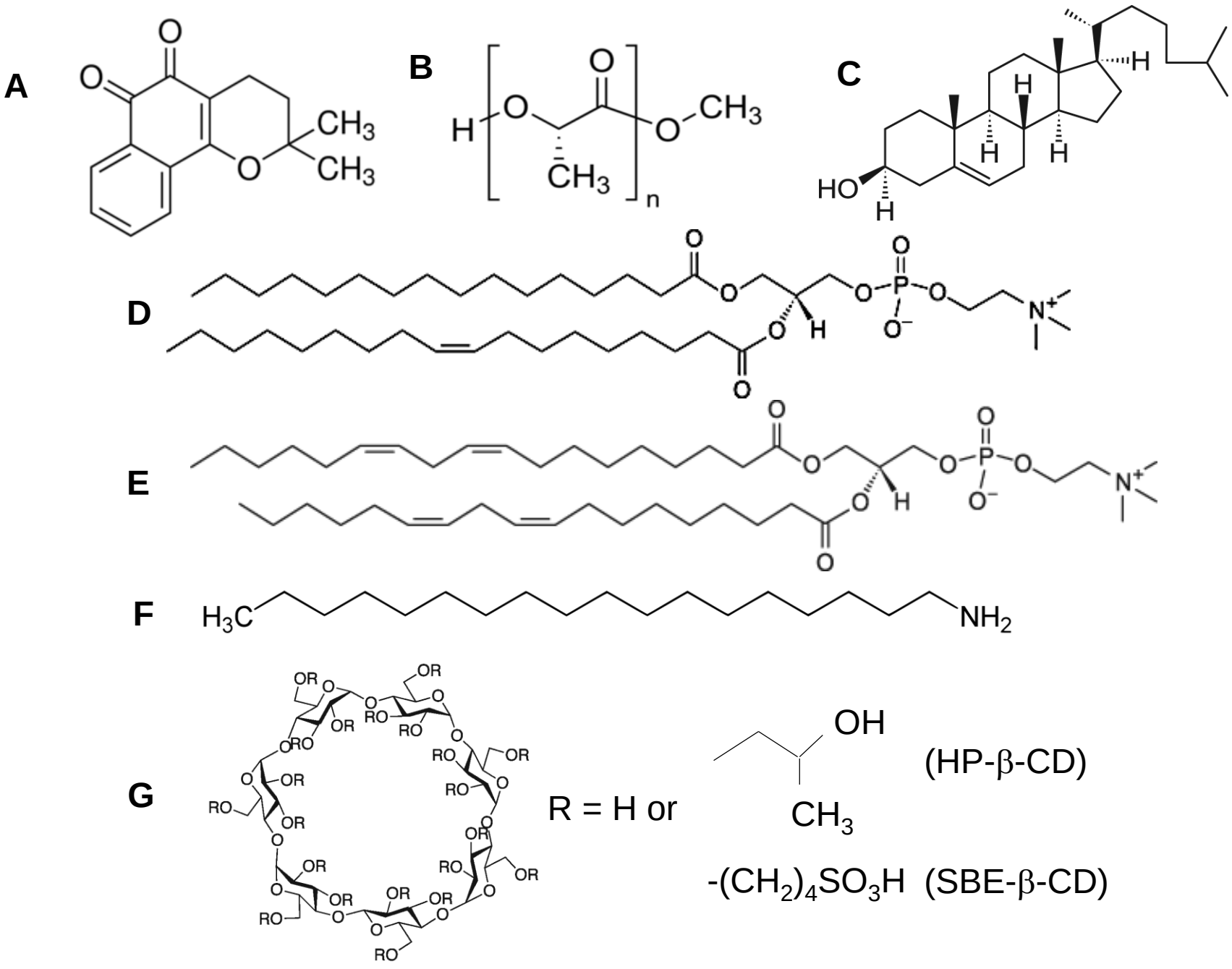
A
B
C
D
E
F
G
R = H or
OH
CH3
(HP-β-CD)
-(CH2)4SO3H (SBE-β-CD)

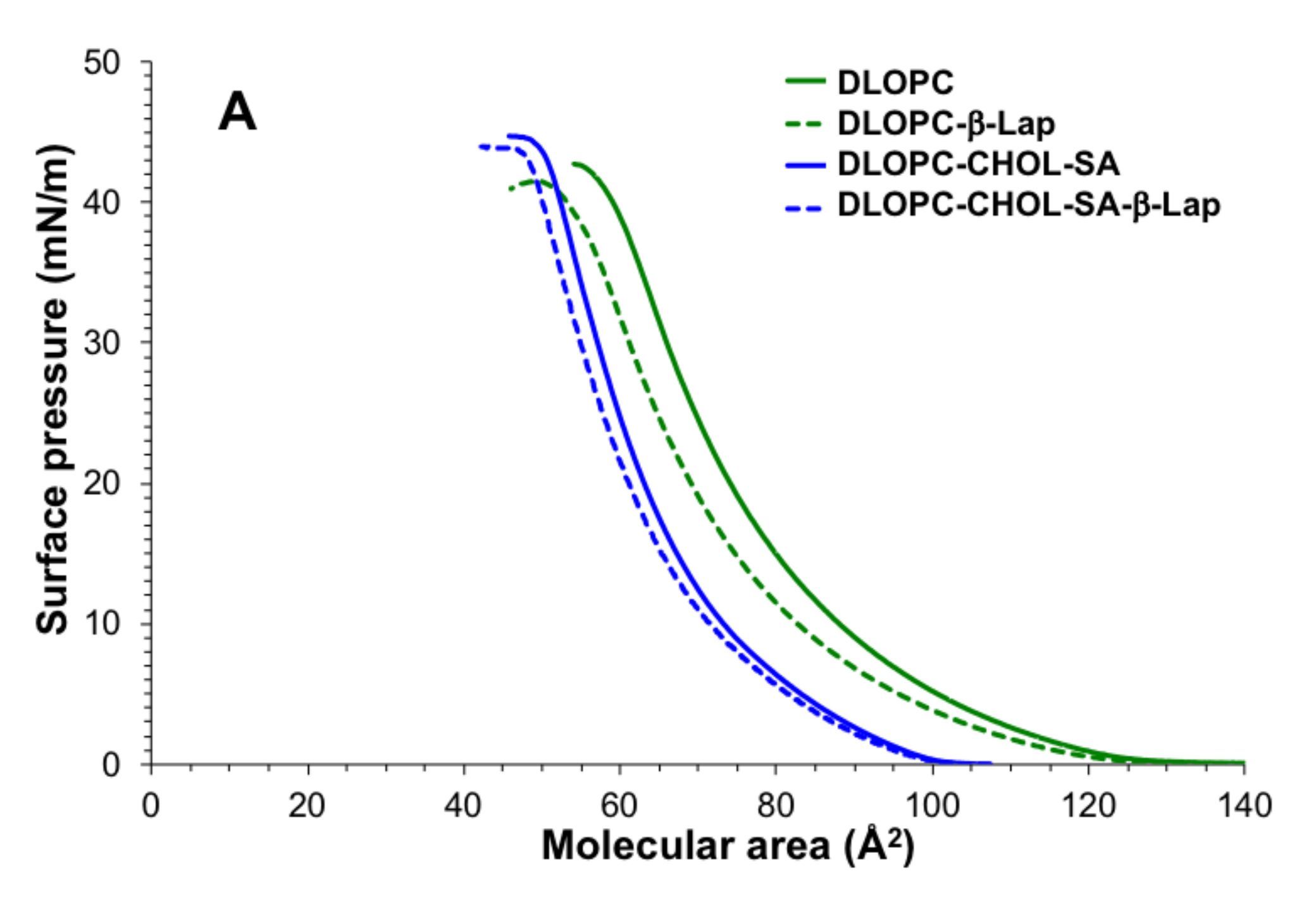
A
DLOPC
DLOPC-β-Lap
DLOPC-CHOL-SA
DLOPC-CHOL-SA-β-Lap
Surface pressure (mN/m)
0
10
20
30
40
50
0
20
40
60
80
100
120
140
Molecular area (Å²)

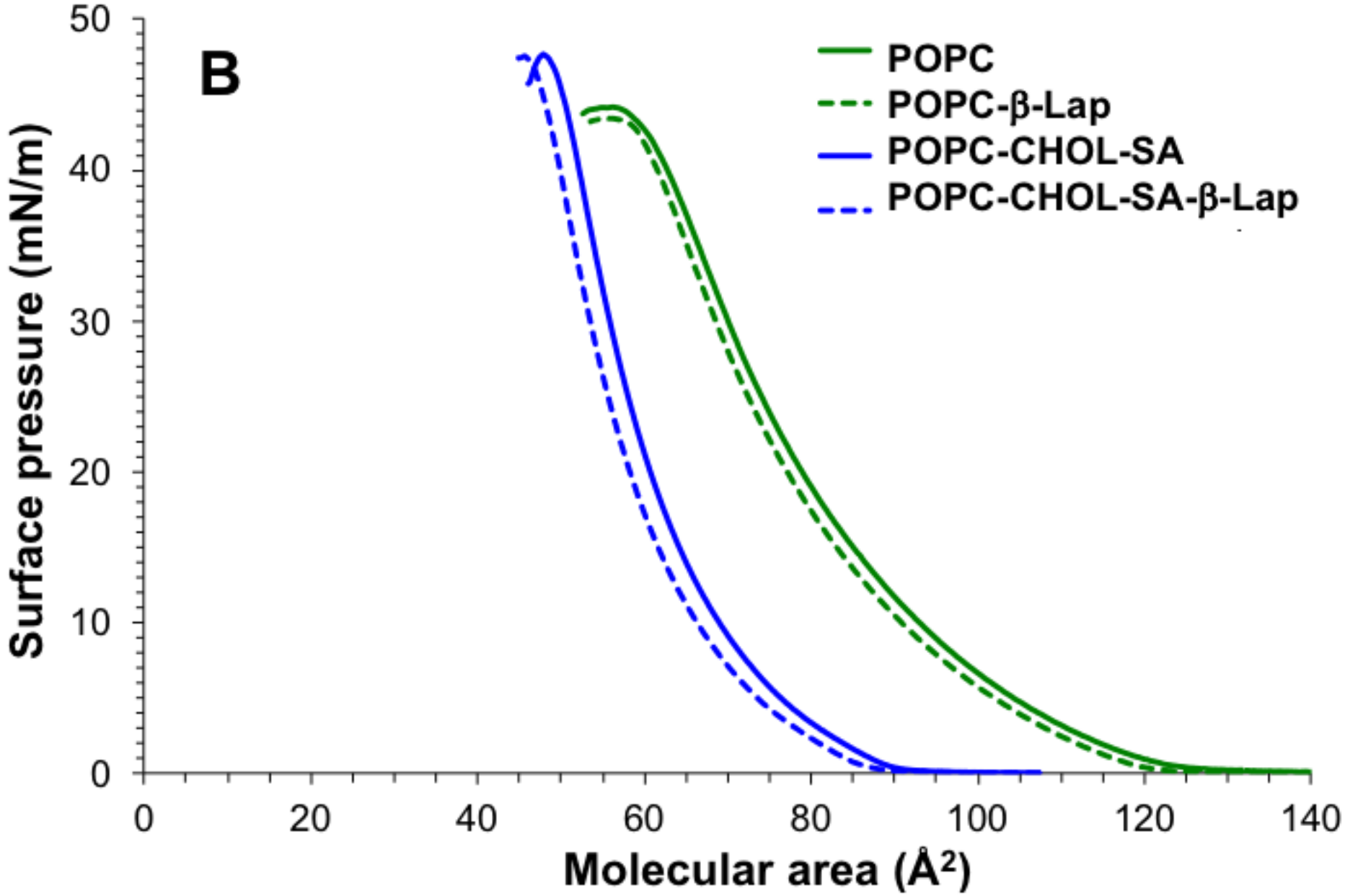
B
POPC
POPC-β-Lap
POPC-CHOL-SA
POPC-CHOL-SA-β-Lap
Surface pressure (mN/m)
0
10
20
30
40
50
0
20
40
60
80
100
120
140
Molecular area (Å²)

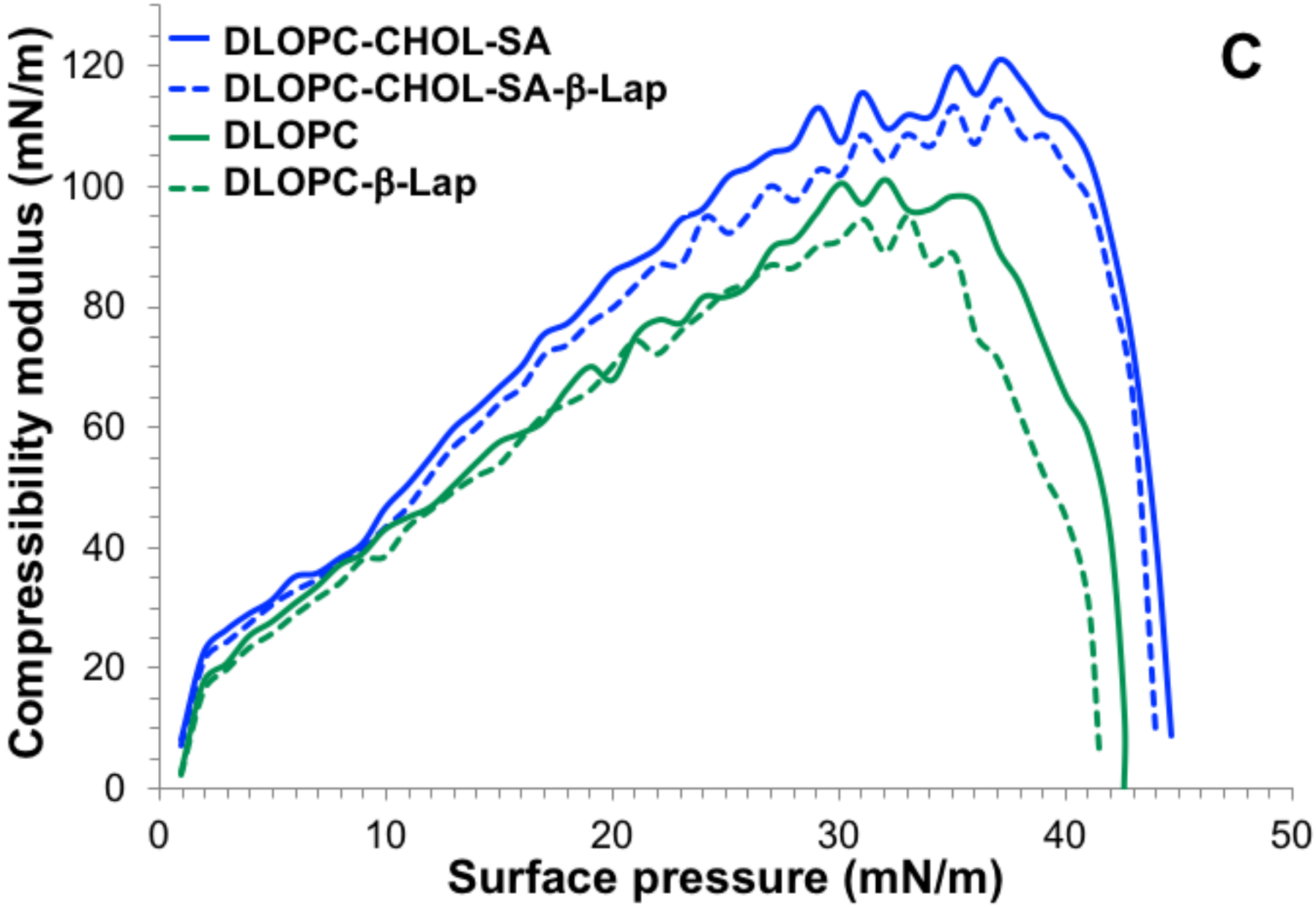
DLOPC-CHOL-SA
DLOPC-CHOL-SA-β-Lap
DLOPC
DLOPC-β-Lap
C
Compressibility modulus (mN/m)
0
20
40
60
80
100
120
0
10
20
30
40
50
Surface pressure (mN/m)

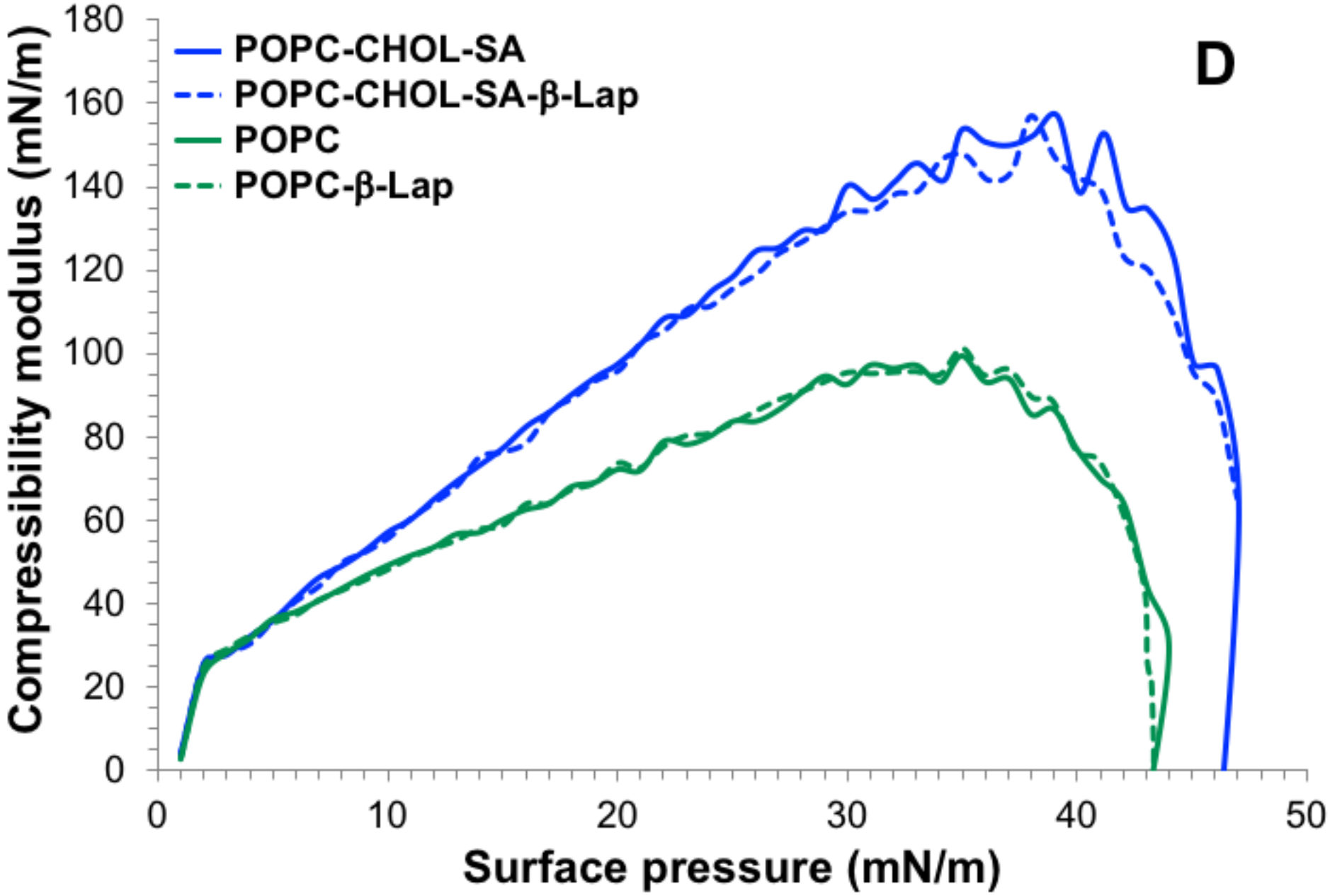
D
POPC-CHOL-SA
POPC-CHOL-SA-β-Lap
POPC
POPC-β-Lap
Compressibility modulus (mN/m)
Surface pressure (mN/m)
0
20
40
60
80
100
120
140
160
180
0
10
20
30
40
50

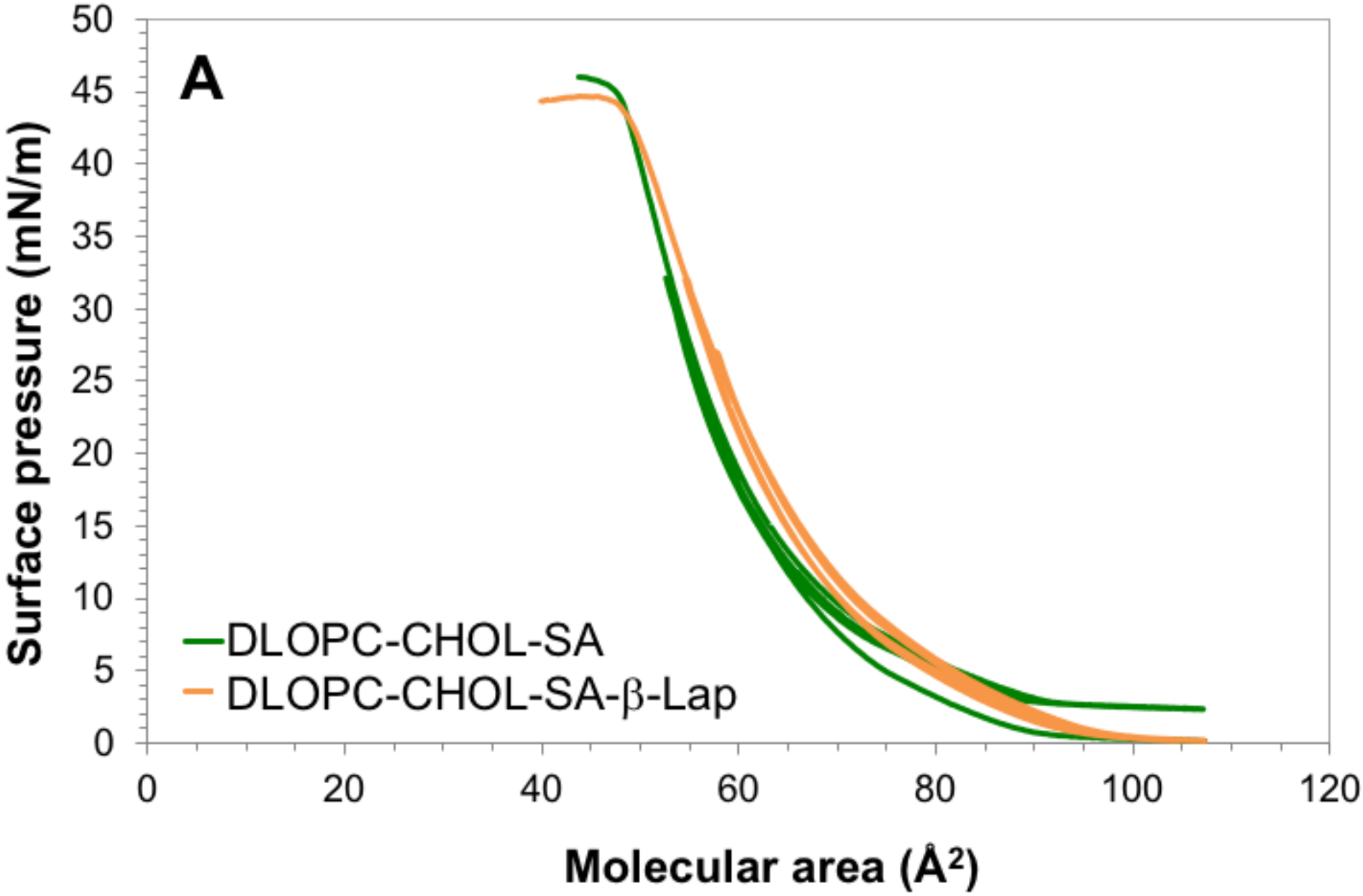
A
Surface pressure (mN/m)
50
45
40
35
30
25
20
15
10
5
0
0
20
40
60
80
100
120
Molecular area (Å²)
DLOPC-CHOL-SA
DLOPC-CHOL-SA-β-Lap

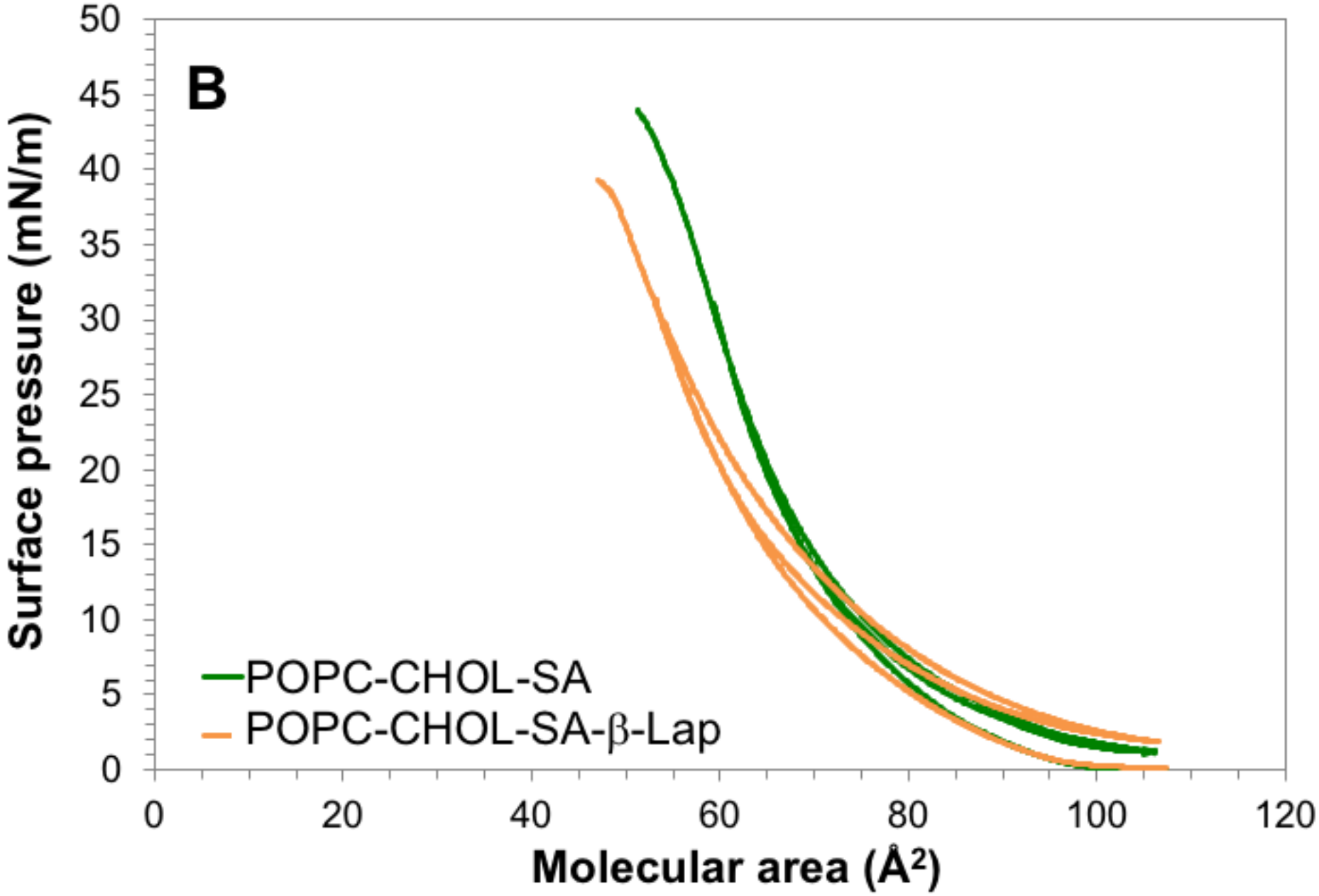
B
Surface pressure (mN/m)
50
45
40
35
30
25
20
15
10
5
0
0
20
40
60
80
100
120
Molecular area (Å²)
POPC-CHOL-SA
POPC-CHOL-SA-β-Lap

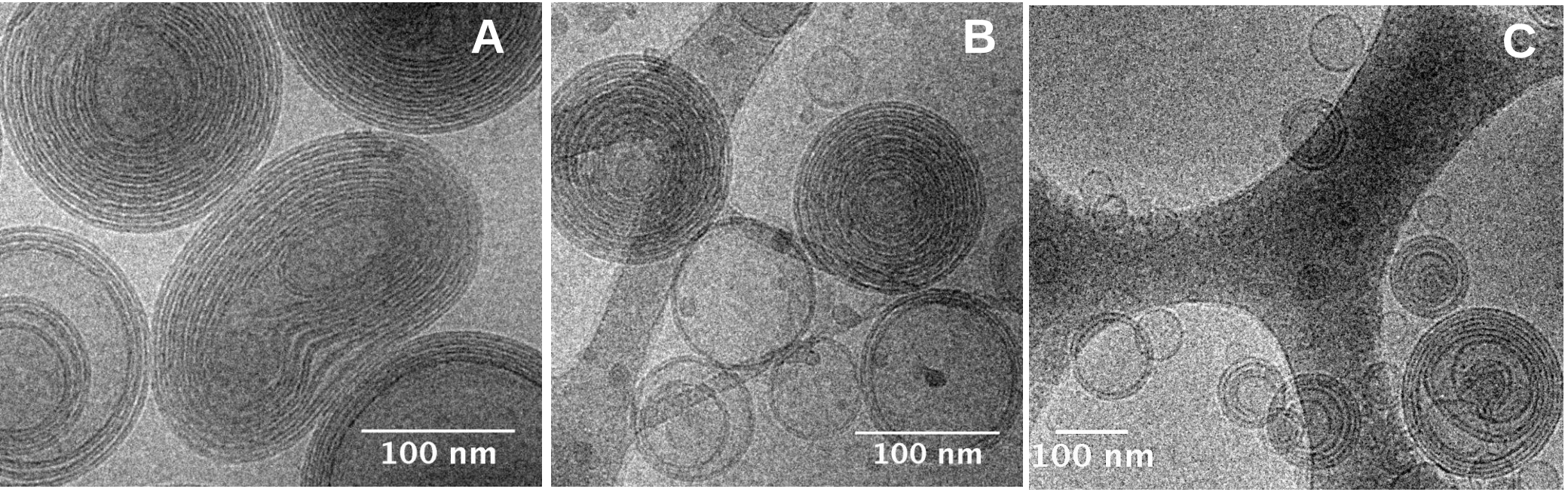
A
100 nm
B
100 nm
C
100 nm

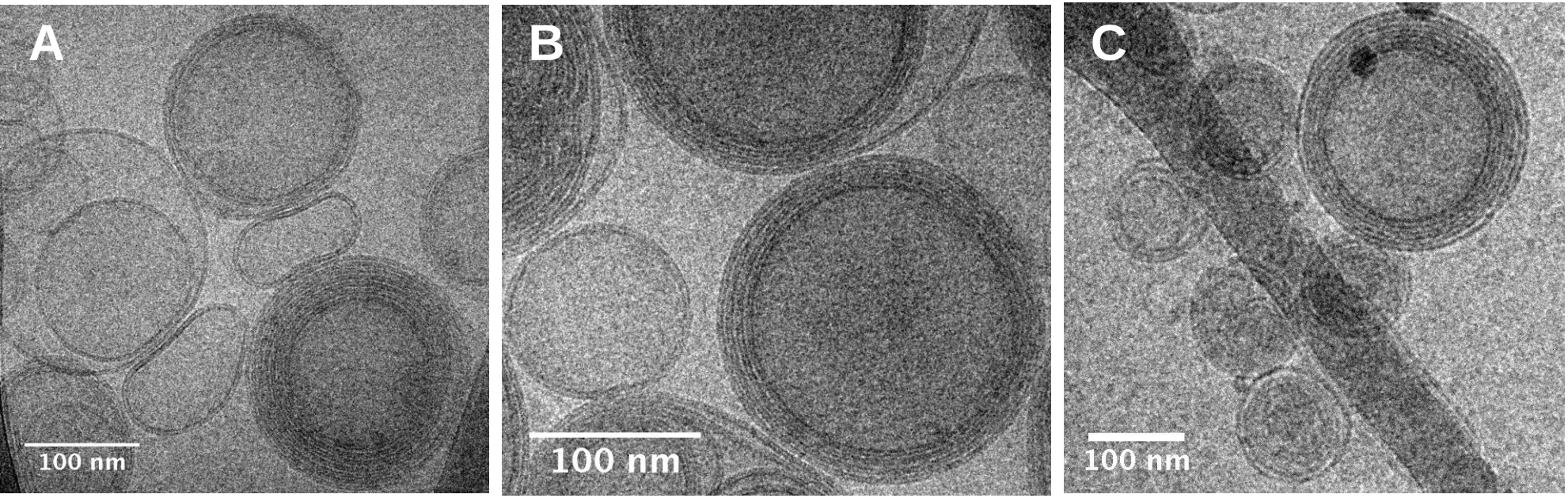
A
100 nm
B
100 nm
C
100 nm

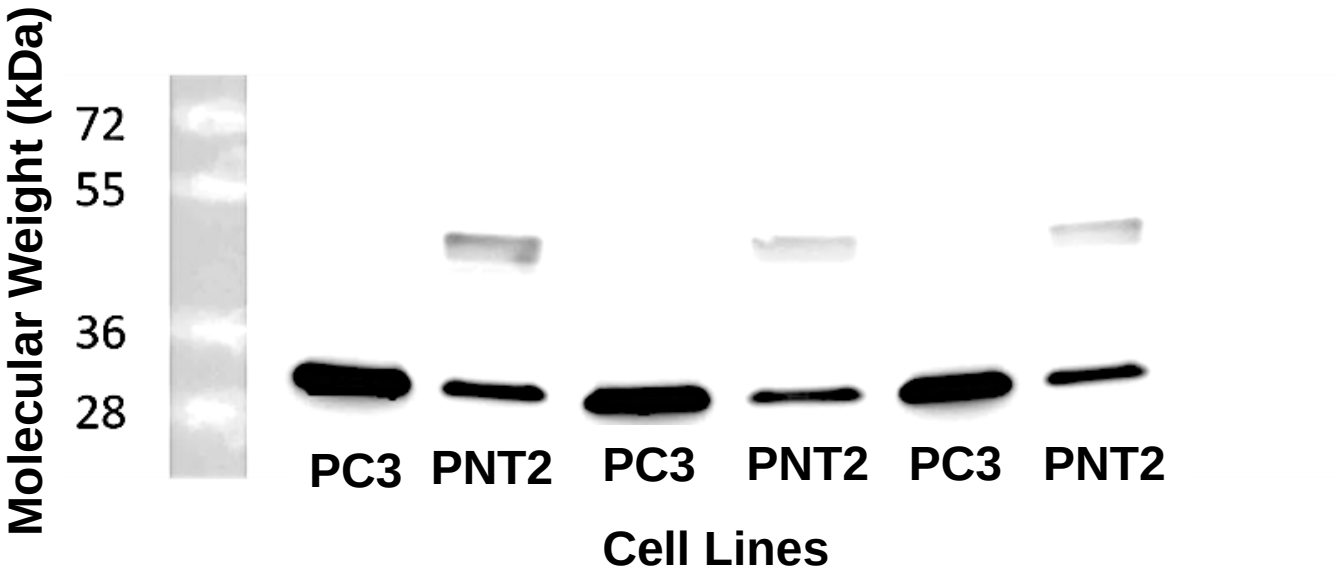
Molecular Weight (kDa)
72
55
36
28
PC3
PNT2
PC3
PNT2
PC3
PNT2
Cell Lines

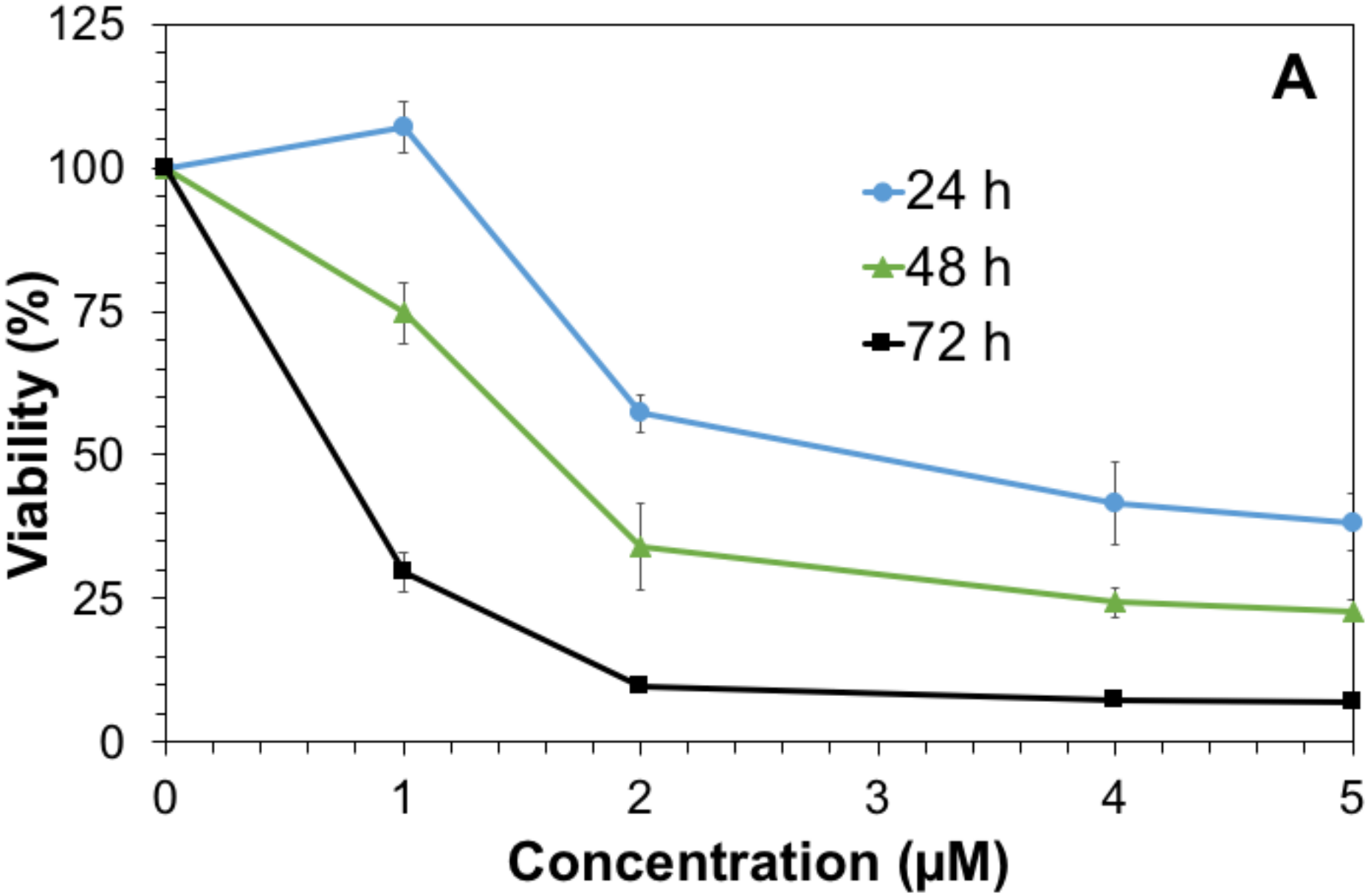
A
125
100
75
50
25
0
Viability (%)
24 h
48 h
72 h
0
1
2
3
4
5
Concentration (μM)

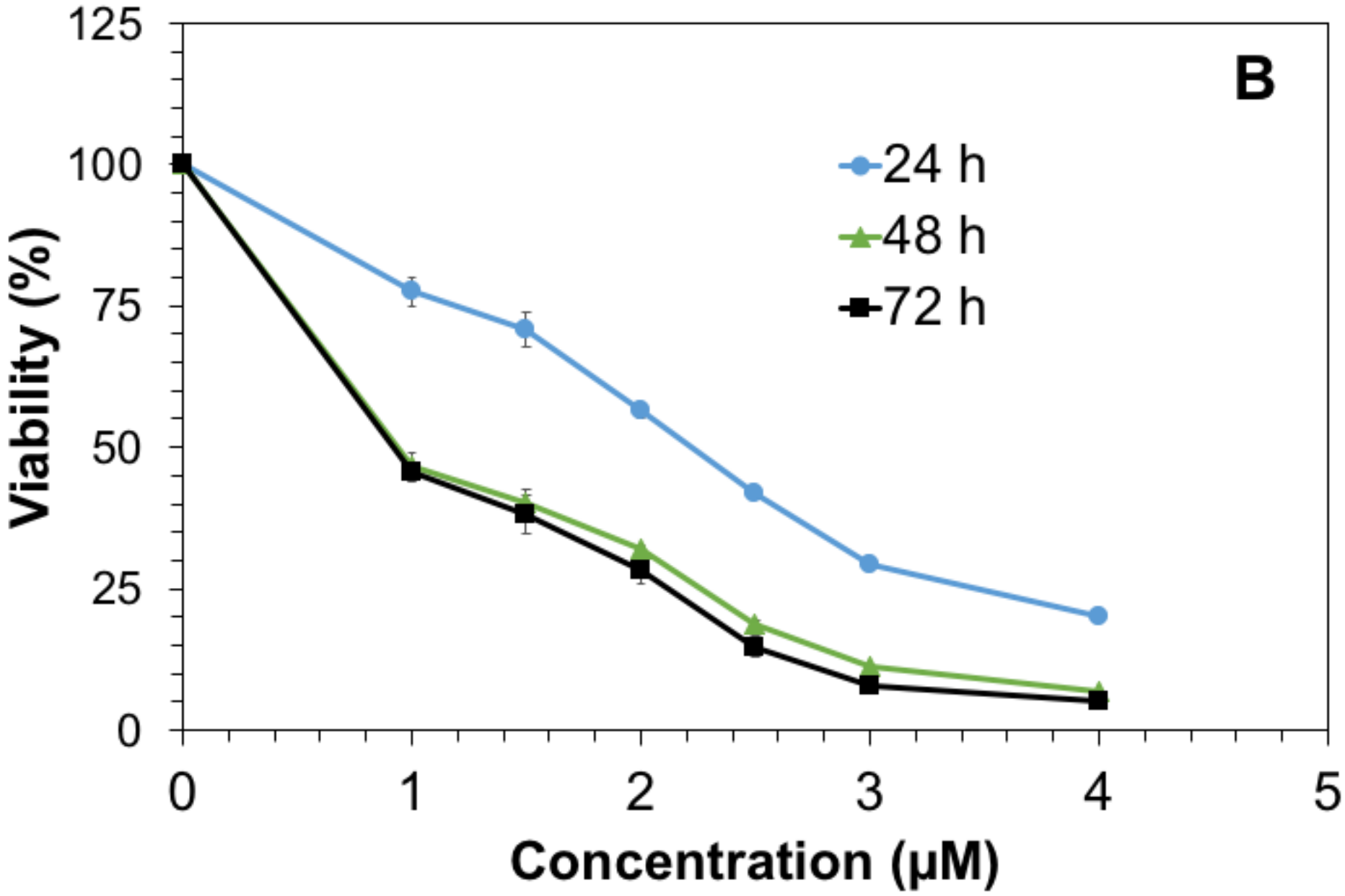
B
24 h
48 h
72 h
Viability (%)
125
100
75
50
25
0
0
1
2
3
4
5
Concentration (μM)

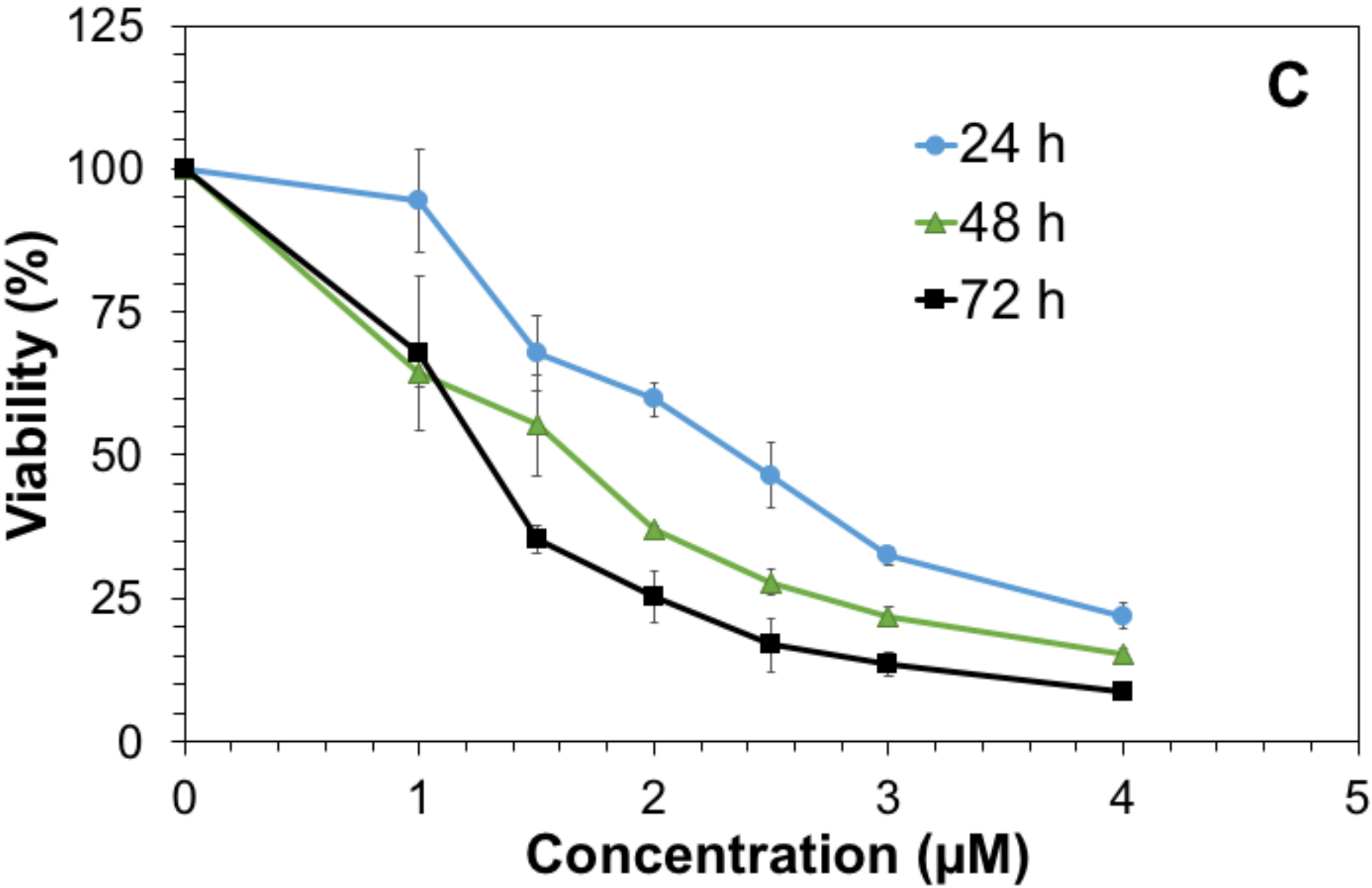
C
24 h
48 h
72 h
Viability (%)
125
100
75
50
25
0
0
1
2
3
4
5
Concentration (μM)

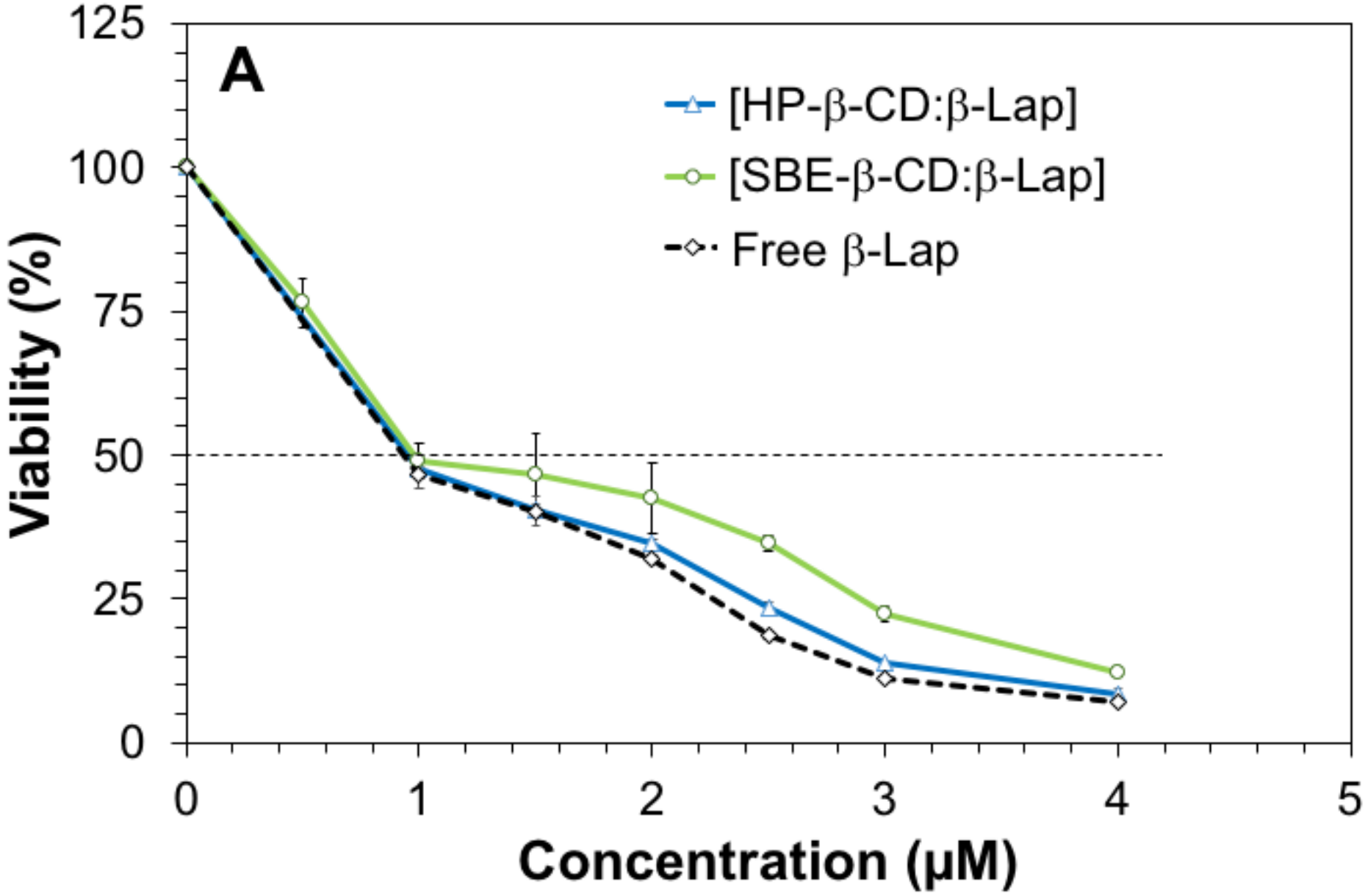
A
[HP-β-CD:β-Lap]
[SBE-β-CD:β-Lap]
Free β-Lap
Viability (%)
125
100
75
50
25
0
0
1
2
3
4
5
Concentration (μM)

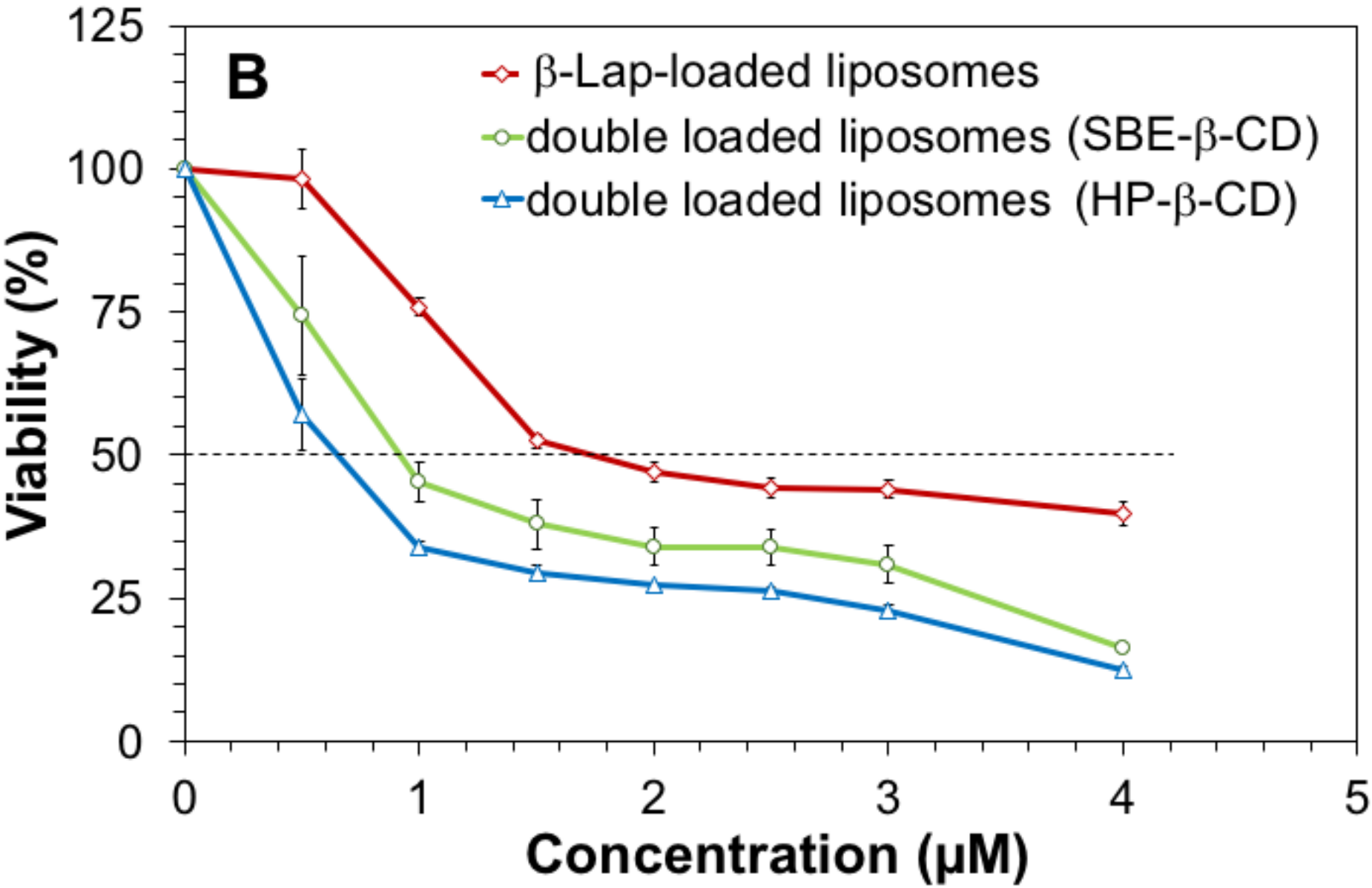
B
β-Lap-loaded liposomes
double loaded liposomes (SBE-β-CD)
double loaded liposomes (HP-β-CD)
Viability (%)
125
100
75
50
25
0
0
1
2
3
4
5
Concentration (μM)

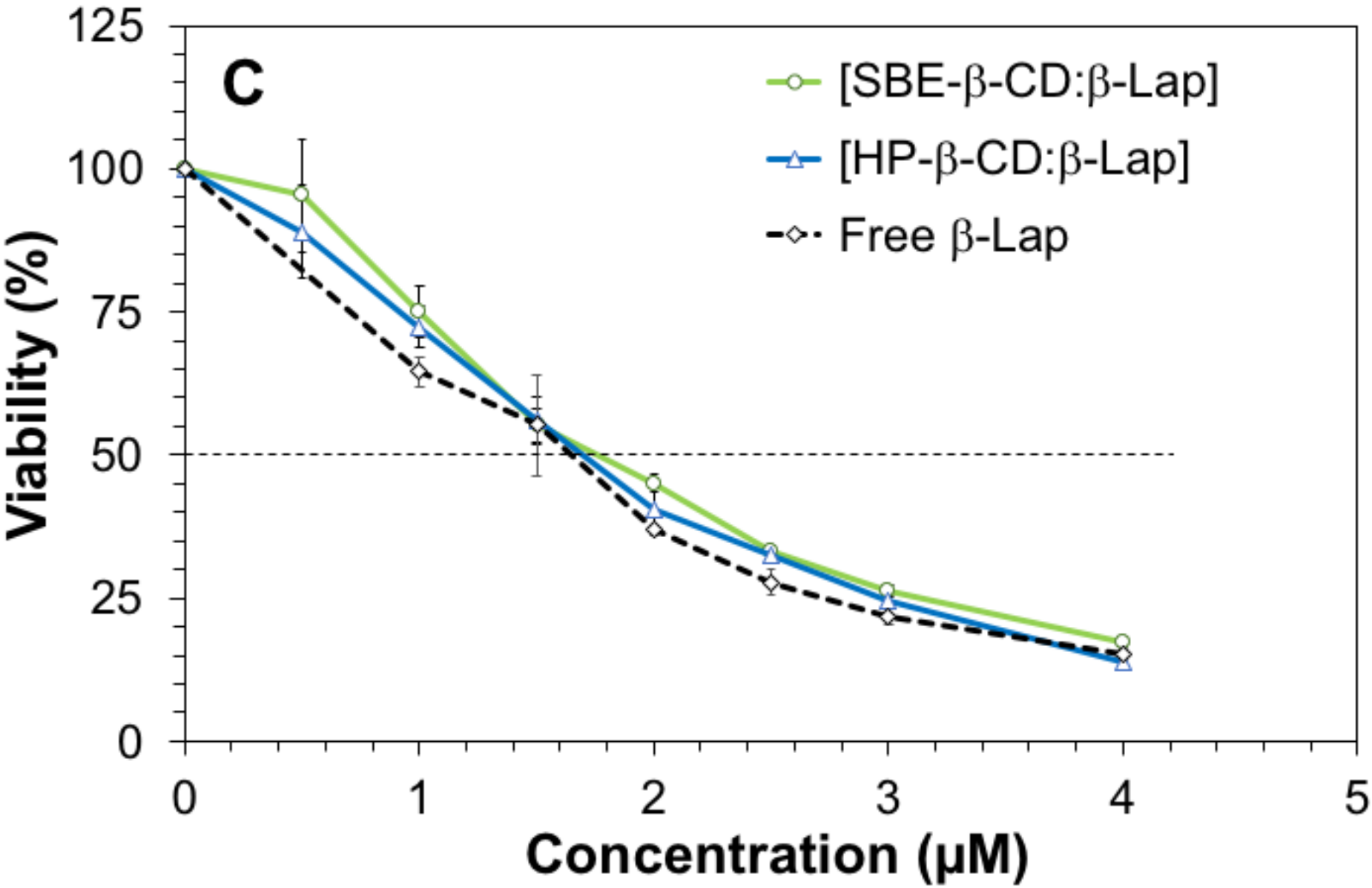
C
[SBE-β-CD:β-Lap]
[HP-β-CD:β-Lap]
Free β-Lap
Viability (%)
125
100
75
50
25
0
0
1
2
3
4
5
Concentration (μM)

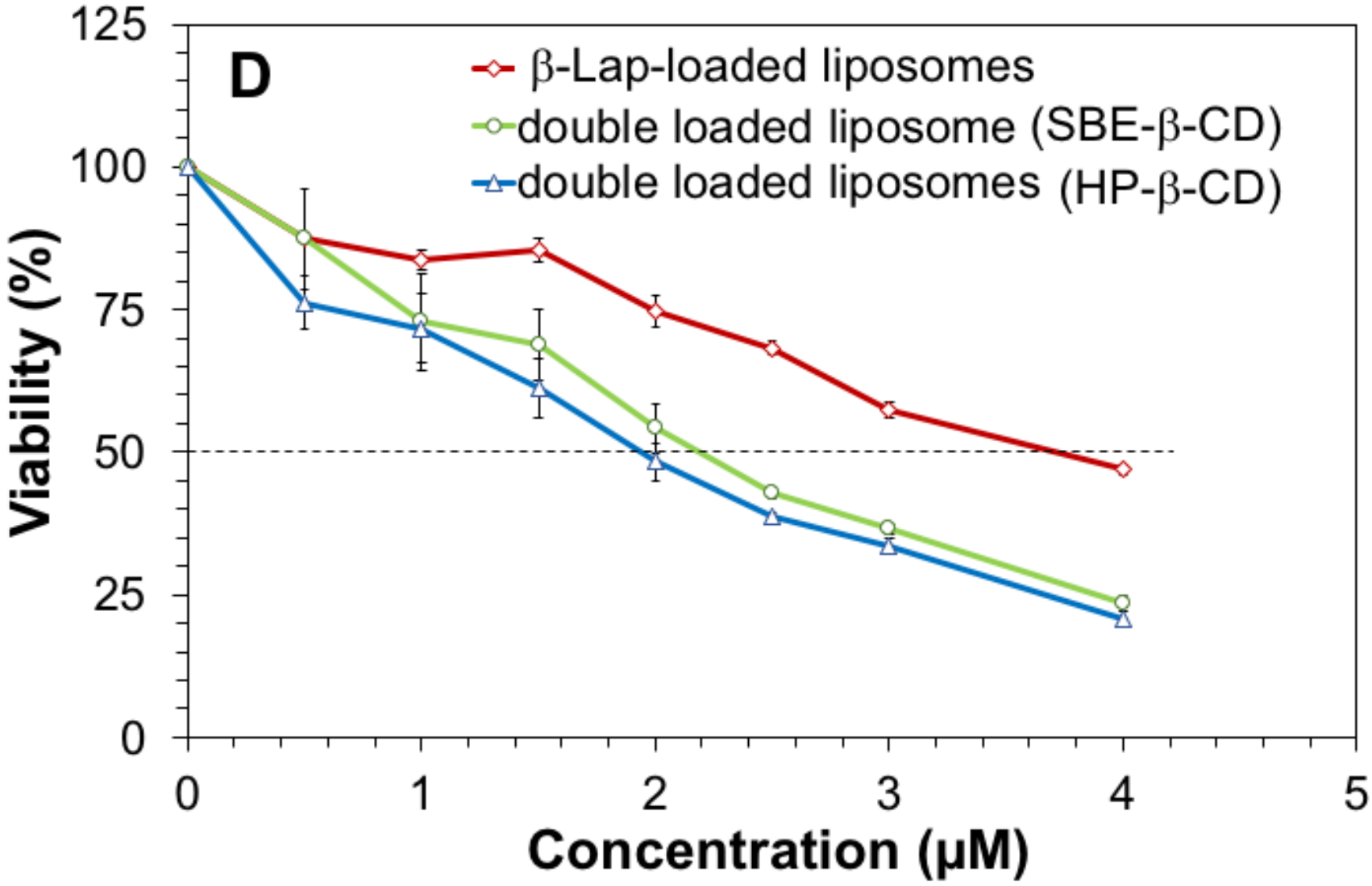
D
β-Lap-loaded liposomes
double loaded liposome (SBE-β-CD)
double loaded liposomes (HP-β-CD)
Viability (%)
125
100
75
50
25
0
0
1
2
3
4
5
Concentration (μM)

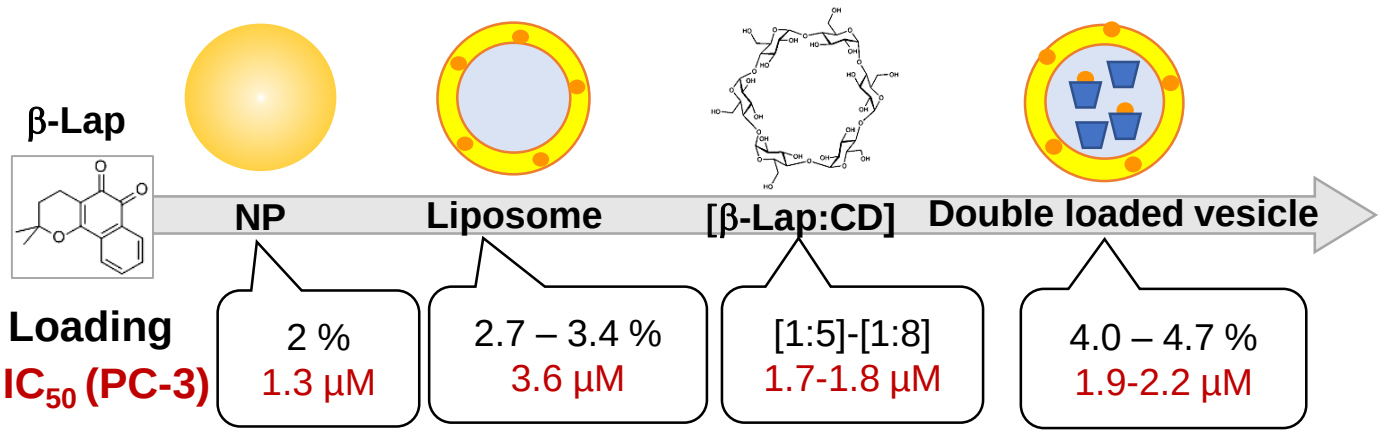
β-Lap
NP
Liposome
[β-Lap:CD]
Double loaded vesicle
Loading
IC50 (PC-3)
2 %
1.3 µM
2.7 – 3.4 %
3.6 µM
[1:5]-[1:8]
1.7-1.8 µM
4.0 – 4.7 %
1.9-2.2 µM